AD-A034 177 UNITED TECHNOLOGIES RESEARCH CENTER EAST HARTFORD CONN F/G 9/5
MODE LOCKED SURFACE ACOUSTIC WAVE OSCILLATOR FOR COHERENT FREQU--ETC(U)
SEP 76 M GILDEN, T M REEDER N66001-76-C-0011
UNCLASSIFIED UTRC-R76-922155-3 NL

1 OF 1
AD
A034177

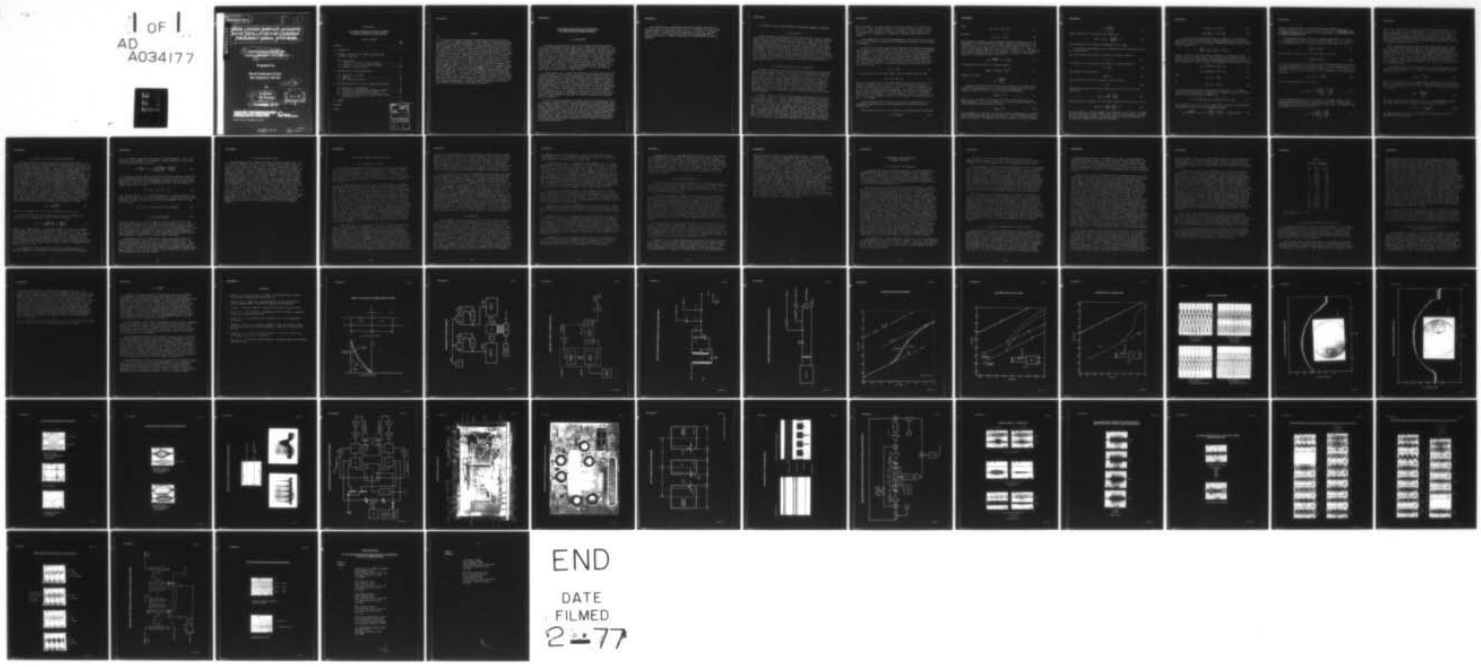

END

DATE
FILMED
2-77

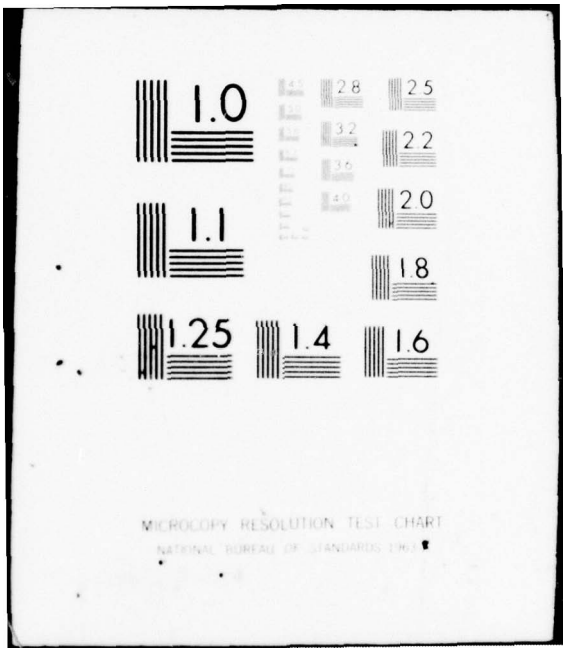
1.0
1.1
1.25
1.4
1.6
2.8
2.5
3.2
2.2
3.6
2.0
4.0
1.8
MICROCOPY RESOLUTION TEST CHART
NATIONAL BUREAU OF STANDARDS 1963

(14) UTRC-R76-922155-3

(6) MODE LOCKED SURFACE ACOUSTIC WAVE OSCILLATOR FOR COHERENT FREQUENCY SIGNAL SYNTHESIS.

(9) Final Technical Report,

Contract N66001-76-C-0011

(15)

Prepared for

Naval Undersea Center
San Diego, Ca. 92132

(12) 57p.

by

(10) M. Gilden
T.M. Reeder

(11) Sept[illegible] 1976

UNITED TECHNOLOGIES RESEARCH CENTER
EAST HARTFORD, CONNECTICUT 06108

76-09-222-1

R76-922155-3

Mode Locked Surface Acoustic Wave Oscillator For Coherent Frequency Signal Synthesis

TABLE OF CONTENTS

ABSTRACT

A new type of frequency synthesizer utilizing Mode Locked SAW oscillators, CZT transducers, and rapidly switchable nonlinear diodes was experimentally demonstrated to be both feasible and promising. The conclusions from this work with a first preliminary model are as follows: The Mode Locked SAW Oscillator (MLSO) is able to provide a set of synchronized and stable short rf pulses with lengths in the range of 50 to 100 nseconds. These pulses can efficiently drive a set of CZT transducers that are used for generating counter flowing SAW discrete chirp signals. By using the sum frequency, signals are synthesized directly at rf frequencies. The Chirp Z Transform approach to frequency synthesis is particularly attractive because it provides means for switching frequencies in a coded sequency within time intervals as short as 50 ns. This was achieved experimentally in the present program. Equally important is the fact that the frequencies are determined only by the physical position of the selected taps. This leads to an additional advantage of this approach in that highly selective filters are not required; commonly available filters can be used for rejecting out of band signals resulting from other nonlinear terms. The results also confirmed that the carrier frequency of the output appears to be fixed only by the CZT transducer geometry and is independent of the input carrier frequencies. The programmable frequency steps are also independent of the input carrier frequencies. Finally, with the use of the coherent and stable pulsed outputs of the Mode Locked SAW Oscillator, generation of coded sequences of frequencies become highly reproducible.

Mode Locked Surface Acoustic Wave Oscillator For Coherent Frequency Signal Synthesis

1.0 INTRODUCTION

This report described the work carried out by United Technologies Research Center on the application of Mode Locked Surface Acoustic Wave Oscillators for the development of coherent frequency signal synthesis techniques. Research under this program was directed toward the development of the UTRC Mode Locked SAW Oscillator (MLSO) (Ref. 1), in a modular form that can be applied to a new, state-of-the-art frequency synthesizer using the Chirp Z Transform which is under study at NUC, (Ref. 2). The goals of this program were three fold: 1) to demonstrate that the broadband pulsed rf output of the MLSO module is stable, coherent, and consistent with theoretical predictions; 2) to design an MLSO module with characteristics suitable for the NUC synthesizer including programmable output frequencies and 3) to fabricate, test, and deliver to NUC an MLSO module based on the design and engineering conclusions reached at UTRC and NUC.

In this program a pair of MLSO's were developed to generate coherent and synchronized rf pulses at two different frequencies. These rf pulses were then used in another SAW component to excite counterflowing discrete-chirp wave forms in a region containing an array of SAW taps. Each tap could be independently turned on through an associated semiconductor diode to provide a "non-linear" cw output at the sum frequency of the two counter flowing chirp signals. The sum frequency is programmable through the selection of the desired SAW tap because the tap position determines the relative timing between the chirp signals. The output signals at the sum frequency, as will be discussed in the text, are not smooth sinusoids. They contain the equivalent of programmable frequencies in the sense that, if the signals are down-converted to base band, the resultant signals are good approximation to sinusoids.

The Chirp Z Transform approach to frequency synthesis is particularly attractive because it provides means for switching frequencies in a coded sequence within time intervals as short as 50 ns. This was achieved experimentally in the present program. Equally important is the fact that the frequencies are determined only by the physical position of the selected taps. This leads to an additional advantage of this approach in that highly selective filters are not required; commonly available filters can be used for rejecting out of band signals resulting from other nonlinear terms. Finally, with the use of the coherent and stable pulsed outputs of the Mode Locked SAW Oscillator, generation of coded sequences of frequencies become highly reproducible.

This report contains a description of frequency synthesis based upon the analysis of discrete chirp waveform in Section 2. A discussion of a pair of synchronized MLSO's and experimental results are given in Section 3. The experimental results on frequency synthesis obtained with the SAW components are presented in Section 4. Finally, conclusions and recommendations are given in Section 5.

2.0 FREQUENCY SYNTHESIS USING DISCRETE CHIRP WAVEFORMS (CHIRPED Z TRANSFORM)

2.1 Introduction

Frequency synthesis techniques using highly stable reference signals, including comb spectra, have been highly developed. In a variety of these techniques frequency mixing, frequency dividing, variable filtering, and phase locking with feed back loops are used extensively (Ref. 3). In most cases, these techniques do not allow for rapidly switching between frequencies as would be required for a coded sequence of frequencies where chip lengths are as short as one microsecond. With the use of SAW concepts, it has now become possible to achieve submicrosecond switching times (Ref. 4) and to select the desired frequency by simply selecting taps electronically in a delay line in which discrete chirped signals are present (Ref. 2). An additional benefit of using SAW components in the scheme to be described in this report is that the individual elements are relatively simple and compact and therefore leads to reduced cost and size.

2.2 Analysis of the Use of the CZT Waveforms

The frequency synthesis technique discussed in this report makes use of counter flowing discrete chirped signals in a SAW delay line. The spatial distributions of two such discrete chirps, at f_1 and f_2, are depicted in Fig. 2-1a for $t = 0$ when the leading edges of the two counter flowing signals are just crossing the axis. The two chirped signals have different carrier frequencies. The output is obtained by mixing these two chirps so that the output may be at either the sum or difference frequency. The output is obtained by the mixing of the signals in nonlinear diodes, that can be switched on or off as desired, at any one of the taps in an array of taps connected to a common output line. In this section, we will discuss how the programmable frequencies are synthesized, what the limitations are and what spurious effects can arise.

The discrete chirp is generated in a SAW Chirped Z Transform Device (CZT) (Ref. 2). The input to the CZT is a train of short synchronized rf pulses at an accurately determined pulse spacing, T. The Mode Locked SAW Oscillator, discussed in Section 3 of this report, provides this type of input to the CZT. The discrete chirp generated by the CZT can be described as a contiguous series of N short rf pulses each with a duration $\tau = T/N$, at some carrier frequency and with abrupt changes in phase between them. These short pulses will be called "chips". The changes in phase along the wave vary such that the accumulated phase is proportional to the square of the distance. The phase changes are produced by exciting two parallel trains of chips with 90 degree phase difference and with amplitude weighting. The amplitude weighting is selected so that when the two quadrature components of a chip are added the desired

phase is obtained. The output from the CZT is also periodic in the distance L or the time T. A most important property of the output of the CZT is that, if there are an even number of chips in the length L (or time T), then the periodic output is equivalent to or approximates a signal for a continuous chirp that goes on forever.

Before formulating the situation mathematically, we will state that the essential features of the synthesis technique can be determined by considering that the chirps are continuous.

The use of the continuous chirp notation simplifies the analysis of the operation and also allows the discrete chirp to be discussed in terms of equivalent continuous chirp parameters as is frequently done in the literature. The justification for this approach is that both the continuous chirp and discrete chirp signals when down-converted to base band (by using the continuous carrier frequency signal as a local oscillator), results in low frequency signals that are similar enough that they can be favorably compared. In the general notation used for traveling waves, the variable in the argument of the function describing the rf chirped SAW pulse must be of the form

$$\theta = \omega t - 2\pi x/\lambda \qquad (1)$$

If the rf in the pulse is linearly chirped, the full argument takes the form

$$\text{Arg} = \theta + a\,\theta^2 + \phi \qquad (2)$$

where a is a constant take to be determined that fixes the range of the chirp. The argument is sketched in Fig. 2-1b at t = 0 for the forward traveling wave as a function of distance for the interval X = -L to X = 0. Both the continuous chirp and the discrete chirp are shown for comparison. The slopes of the discrete steps are all constant and parallel to the dashed linear curve, which is the constant frequency line corresponding to the carrier frequency. With the notation used in Eqs. (1) and (2), the variable X will be used to designate a tap position where the wave is to be sampled.

The relationships between the range of the chirp, the maximum range of the programmable signal frequencies, and the parameters of the SAW device will be discussed next.

We will define the function F to represent the traveling chirped SAW waveform;

$$F = A\ \text{Exp}\ j[\text{Arg}] \qquad (3)$$

where

$$Arg = \theta_i + a_i \theta_i^2 + \phi_i \tag{4}$$

and where

$$\theta_i = \omega_i t - 2\pi x/\lambda_i \tag{5}$$

The subscript i, designates a carrier frequencies under discussion and λ_i is the wavelength. The basic interval of the chirped signal will be defined at t = 0 as extending from X = -L to X = 0, where L is the spatial length of the chirped SAW signal on the crystal surface and is selected to be a multiple of λ_i. Thus, at t = 0 the corresponding range for θ extends from $\theta = -2\pi L/\lambda_i$ to $\theta = 0$. An arbitrary phase constant is allowed for by ϕ. The equivalent instantaneous chirp angular frequency is determined from Eqs. (4) and (5),

$$\omega_{ci} = \frac{d(Arg)}{dt} = \omega_i + 2a_i\omega_i\theta_i \tag{6}$$

The maximum frequency change in the chirp frequency is

$$\Delta\omega_{max} = 2a_i\omega_i\theta_{max} = 2a_i\omega_i^2 T \tag{7}$$

Therefore, in general

$$a_i = \frac{\Delta\omega_{max} T}{2\omega_i^2 T^2} \tag{8}$$

Graphical consideration of how the two counterflowing discrete chirp signals interact at various tap positions, x, shows that the maximum range for the programmable frequency deviation at the sum or difference frequency is

$$\Delta\omega_{p\,max} = 2\pi f_c \tag{9}$$

where $f_c = 1/\tau$ and where τ is the length of a chip. We will also call f_c the sampling frequency. Further consideration of the discrete frequency chirps themselves indicates that with respect to Eq. (8)

$$\Delta\omega_{max} = 2\pi f_c \tag{10}$$

These statements are based upon the fact that at base band frequencies, the highest modulation frequency could only have a period of τ. With the relationships given in Eqs. (9) and (10), the expression for the slope constant, a_i, in Eq. 8, becomes

$$a_i = \frac{\pi f_c T}{(\omega_i T)^2} \tag{11}$$

Finally, from Eq. (4), the argument can be written as

$$\text{Arg} = \theta + \pi f_c T \left(\frac{\theta_i}{\omega_i T}\right)^2 + \phi \tag{12}$$

with the variable of the chirped term normalized to $\omega_i T = \theta_{max}$.

The discrete chirp parameters can be introduced for use in the second term of Eq. (12) as follows:

The discrete time values using n, an integer, as a running variable is

$$t_n = n\tau \tag{13}$$

The discrete space values using m, an integer, as a running variable is

$$x_m = m\Delta x \tag{14}$$

The increment, Δx is defined by,

$$2N\Delta x = L \tag{15}$$

where the number of chips in the chirp is N and is defined by

$$N\tau = T \tag{16}$$

Finally, we can write for the discrete values of θ in Eq. (12) for use in the second term

$$\theta_{mn} = \omega_i T \left(\frac{n}{N} - \frac{1}{2}\frac{m}{N}\right) \tag{17}$$

Equation (12) can be expressed for the discrete chirp, with the help of Eq. (9), as

$$\text{Arg} = \theta + \pi N \left(\frac{n}{N} - \frac{m}{2N}\right)^2 + \phi \tag{18}$$

The first term in Eq. (18) with respect to the function F of Eq. (3), is a continuous function generating a constant frequency while the second term generates the chirp which has only discrete values. The discrete values of n and m are determined as the continuous variables that satisfy the conditions:

$$n \text{ for } n\tau < t < (n+1)\tau \tag{19}$$

$$m \text{ for } m\frac{L}{2N} < x < (m+1)\frac{L}{2N} \tag{20}$$

In order to determine what factors effect the character of the frequency synthesized signals, we will continue a general analysis with continuous chirps in this section. For the continuous chirp, the instantaneous frequency from the traveling wave formulation is:

$$\omega = \frac{d\text{Arg}}{dt} = \omega_i[1 + 2a_i(\omega_i t - 2\pi\, x/\lambda_i)] \tag{21}$$

From Eq. (21), we note that the function describing the instantaneous angular frequency is also a traveling wave. This expression does not apply directly to the discrete chirp. For counter flowing chirped SAW signals, having frequencies f_1 and f_2, that would be used to generate the programmable output signals, we can write

$$F_1 = A_i \text{Exp}\, j[\theta_1 + a_1\, \theta_1^2 + \phi_1] \tag{22}$$

$$F_2 = A_2 \text{Exp}\, j[\theta_2 + a_2\, \theta_2^2 + \phi_2] \tag{23}$$

where

$$\theta_1 = \omega_1 t - 2\pi x/\lambda_1 \tag{24}$$

and

$$\theta_2 = \omega_2 t - 2\pi x/\lambda_2 \tag{25}$$

The slope constants are allowed to be arbitrary at this point. The nonlinear signal output corresponding to the product of the signals F_1 and F_2 at some fixed position X where the two waves are sampled, is

$$S = \eta\, A_1 A_2 \text{Exp}\, j[\theta_1 \pm \theta_2 + a_1\, \theta_1^2 \pm a_2\, \theta_2^2 + \phi_1 \pm \phi_2] \tag{26}$$

Then substituting Eqs. (24) and (25) into Eq. (26) and taking the time derivative an expression is obtained for the programmable frequency

$$\omega_p = \frac{d\ \text{Arg}(S)}{dt} = \omega_1 \pm \omega_2 - 4\pi\left(\frac{a_1\omega_1}{\lambda_1} \pm \frac{a_2\omega_2}{\lambda_2}\right) x + 2(a_1\omega_1^2 \pm a_2\omega_2^2)\, t \tag{27}$$

The upper signs corresponds to the sum frequency and the lower signs to the difference frequency. The second term in Eq. (27) represents a programmable shift in frequency proportional to x while the third term represents an undesirable chirp contribution independent of x.

The programmable frequency shift with x is made maximum when $a_1 > 0$, if for the sum frequency, $a_2 > 0$, and if for the difference frequency $a_2 < 0$. Fortunately, the undesirable chirp term, for the above conditions, can be made to vanish if

$$|a_1|\omega_1^2 \equiv |a_2|\omega_2^2 \tag{28}$$

for all values of ω_1 and ω_2 (as is the case for the CZT) or if

$$|a_1|\omega_{01}^2 \equiv |a_2|\omega_{02}^2 \tag{29}$$

In Eq. (29) ω_{01} and ω_{02} are the specific reference angular frequencies that are used to define the relationship between $|a_1|$ and $|a_2|$. The desired expressions for the programmable frequencies can be obtained by substituting Eq. (28) or (29) into Eq. (27) and by using the other conditions given in this paragraph. The desired expressions are:

$$\omega_p = \omega_1 \pm \omega_2 - 4a_1\omega_1^2\frac{x}{v} \tag{30}$$

for the condition expressed by Eq. (28) and

$$\omega_p = \omega_1 \pm \omega_2 - 2a\omega_{01}^2\left(\frac{\omega_1^2}{\omega_{01}^2} + \frac{\omega_2^2}{\omega_{02}^2}\right)\frac{x}{v} \tag{31}$$

for the conditions expressed by Eq. (29), where v is the phase velocity. The x frequency relationships expressed by Eqs. (30) and (31), while depending upon x, are independent of whether the sum or difference term is used. The undesired chirp term becomes either zero, for Eq. (28) or

$$\omega_t = a\omega_{01}^2\left(\frac{\omega_1^2}{\omega_{01}^2} - \frac{\omega_2^2}{\omega_{02}^2}\right)t \tag{32}$$

for Eq. (29). Equation (32) is seen to vanish at the reference frequencies, i.e., when $\omega_1 = \omega_{01}$ and $\omega_2 = \omega_{02}$ simultaneously. It is evident that Eqs. (30), (31), and (32) also apply if $a_1 < 0$. The conditions on the signs of a_1 and a_2 given earlier in this paragraph also define the relative directions of the chirps. For the sum frequency, the spatial variation of the chirps are in the same direction, while for the difference frequency the chirps are in opposite directions. This can be determined by reference to Eq. (6).

The CZT transducer generates a discrete chirp signal by providing a sequence of rf chips with abrupt changes in phase such that the accumulated variation in phase equals that of the quadric component in the equivalent continuous linear chirp, Eq. (2) and Fig. 1b. Since the changes in phase are only determined by the physical design of elements in the Chirp Z Transform SAW transducer, these discrete chirps at f_1 and f_2 can be made to have the same accumulated phase variation by using identical transducer lengths, tap numbers, tap spacing and tap weighting. The consequence of this choice in design is that the condition given in Eq. (28) is satisfied automatically.

Additional insight and design information can be obtained by using Eq. (30) to rederive an expression for a_1. Let $\Delta\omega_{pmax}$ be the maximum programmable frequency range when $x = L/2$. Then

$$\Delta\omega_{pmax} = 2a_1\omega_1^2 T \tag{33}$$

where T is the time duration of the chirped pulse. The value L/2 is substituted into Eq. (30) because the counter flowing CZT SAW waveforms will overlap identically within a spatial periodicity of L/2. Thus, the chirp coefficients introduced in Eq. (6) becomes

$$|a_i| = \frac{\pi(\Delta f_{pmax})T}{\omega_i^2 T^2} \tag{34}$$

This result confirms the statement made in Eq. (8). The programmable equivalent frequencies from the discrete chirps can be written from Eq. (30) as

$$f_m = f_1 \pm f_2 - (\Delta f_{pmax})\frac{m}{N} \tag{35}$$

by using the definitions of Eqs. (13) through (16), where m goes from 0 to N to cover all of the tap positions.

2.3 Analysis of the Effect of Carrier Frequencies

Other input frequency dependent terms must be considered with respect to the waveform generated by the CZT transducer when the frequencies are to be varied. The important terms for frequency synthesis are those for the discrete chirps that give rise to the sequence of short rf "chips". There are abrupt phase changes from chip to chip such that the accumulated phase at the nth chip is proportional to n^2. These phase changes are provided for by the weighting of the quadrature finger sets in the CZT transducer where each finger set generates one chip of the sequence. The other term which must be considered also produce abrupt phase changes from chip to chip. The source of these additional phase changes can be understood by observing that the weighted finger sets in an ideal CZT transducer are spaced by an integer number of wavelengths. Furthermore, the CZT transducer is pulsed with an rf pulse that is essentially equal in length to the spacing between the finger sets under ideal conditions. Therefore, at the center frequency of the CZT transducer, if the weighting of the finger sets are constant, a continuous and smooth sinusoidal rf waveform would be generated. However, if the rf frequency of the applied pulses is different than the center frequency, the resultant rf waveform is no longer continuous. This occurs because a finger set of the CZT will generate an rf waveform for a single chip, whose length is no longer a multiple of a wavelength. In fact, the deviation from a multiple of a wavelength can be expressed as an angle

$$\Delta\theta_f = \theta_{O\tau}\left(\frac{f-f_O}{f}\right) \tag{36}$$

where $\theta_{O\tau}$ is a multiple of 2π at the center frequency (i.e., $\theta_{O\tau} = \omega_O\tau$).

The contribution to the total argument used to define the traveling wave generated by a CZT transducer (see Eqs. (12) and (18)) becomes:

$$\text{Arg} = \theta - \theta_{O\tau}\left(\frac{f-f_O}{f}\right)\frac{\theta_n}{\theta_\tau} + \pi N\left(\frac{\theta_n}{N\theta_\tau}\right)^2 \tag{37}$$

where $\theta = \omega t - 2\pi\frac{x}{\lambda}$ and where θ_τ is the spacing between the finger sets in radians at the particular input frequency of the pulsed rf, denoted as f. The second term occurs because the spacing between finger sets, in general, is not an exact multiple of 2π radians and the third term is the discrete chirp term. Only at the center frequency, f_o, does this term not make any contribution. The subscript n is used in the second and third terms, as was done before, to denote that θ_n/θ_τ takes on only integer values n as the continuous variable θ passes through the corresponding intervals $n\theta_\tau < \theta < (n+1)\,\theta_2$.

The significance of the second term can be seen by considering next the equivalent expression for the argument in continuous form, since this form allows

the use of explicit expressions for equivalent signal frequencies. Thus, the time derivative of the argument of the equivalent continuous signal of Eq. (37) gives for the instantaneous chirp frequency

$$\omega = \frac{d(Arg)}{dt} = \omega_1 - \theta_{O\tau}\left(\frac{f_1 - f_{O1}}{f_{O1}}\right)\frac{\omega_1}{\theta_\tau} + \frac{\omega_c}{2}\left(\frac{\theta_1}{N\theta_\tau}\right) \tag{38}$$

In the frequency synthesis process, either sum or difference frequency terms of the two counterflowing chirped SAW's are utilized. The second term in Eq. (38), when applied in the derivation of the programmable frequencies from the counter flowing chirped SAW's, would given an additional frequency offset term, when reduced to simplest form, as given below:

$$\delta f = -(f_1 - f_{O1}) \pm (f_2 - f_{O2}) \tag{39}$$

These terms add linearly to the other term generated by the chirp components. The upper sign correspond to using the sum frequency and the lower term to the difference frequency. The full expression for the equivalent programmable frequencies from Eq. (35) becomes:

$$f_m = f_1 \pm f_2 - (f_1 - f_{O1}) \pm (f_2 - f_{O2}) - (\Delta f_{max})\frac{m}{N} \tag{40}$$

or

$$f_m = f_{O1} \pm f_{O2} - (\Delta f_{max})\frac{m}{n} \tag{41}$$

The result expressed by Eq. (41) is unexpected as it indicates that the output signal carrier is independent of the input carrier frequencies f_1 and f_2. Thus, if the output is converted to base band using $f_1 \pm f_2$ as a local oscillator signal, there would be an off-set in frequency given by the terms in parentheses in Eq. (40). This last observation is important for aiding in interpreting the experimental results, because in our experiments, a synchronous local oscillator signal was used that corresponds to mixing f_1 and f_2, the two carrier frequencies.

This analysis, since it is based upon an assumed equivalence between the continuous and discrete chirp, does not give a completely accurate result. The chirped pulse waveform from the CZT has even symmetry about the mid-point. Therefore, the resultant output waveform should also have even symmetry with respect to the tap region. This implies that only one half of the programmable frequency range, Δf_{max} in Eq. (41), can be obtained or that the useful range for m is only 0 to N/2. The experimental results show this behavior.

2.4 Frequency Synthesis Circuit

The block diagram for the frequency synthesis technique is shown in Fig. 2-2. The detailed discussion in Section 2.2 above, explained how the chirp section, the tap region and the nonlinear mixing generate the desired programmable frequency signals. Because the length of the steps in the argument (Fig. 2-1) are large compared to an rf cycle, the output signals are not readily recognized as having programmable frequencies. However, if the output signals are down-converted to base band where the length of the step are now small compared to the sinusoidal period, the programmable frequencies do become evident. In Fig. 2-2 each of the discrete chirp ROM's performing the CZT launch the pair of counterflowing chirped signals. The nonlinear operation providing the sum or difference frequency from the desired tap is accomplished by causing the diode in series with that tap and the output bus to be biased to an optimum current bias value. The frequency select function consists of connecting the desired diode to the "on" bias bus. Each of the chirp sections is driven by a mode locked SAW oscillator (discussed in detail in Section 3) which provides a short coherent rf pulse. The two mode locked oscillators are synchronized to a common trigger source. In order to contain the diodes in a closely spaced array that would match the tap spacing, as would be required in a practical application, the diode block in Fig. 2-2 represents an array of diodes that we fabricated using integrated circuit techniques on an SOS (silicon on sapphire) substrate.

3.0 THE MODE LOCKED SAW OSCILLATOR (MLSO)

3.1 Description of the MLSO

The Mode Locked SAW Oscillator (MLSO) is a new type of pulsed radio frequency oscillator invented by UTRC prior to the initiation of this program. The MLSO inherently has a high degree of coherence and stability. It is analogous to the microwave frequency regenerative pulsed oscillator of Cutler (Ref. 15) and to the mode locked lasers of Hargrove (Ref. 6) and DeMaria (Ref. 7). The MLSO is made possible because of the basic characteristics found in the delay line controlled, CW, SAW oscillator (Ref. 8).

The CW single-frequency SAW oscillator is a classical example of a feedback amplifier that uses a SAW delay line to provide the positive feedback signal. The oscillator is illustrated by the circuit shown in Fig. 3.1 with the expander component bypassed. Since the insertion loss of typical delay lines is of the order of 20 to 30 dB, a large feedback ratio is not available. One significant characteristic of this SAW oscillator, resulting from the relatively long time delays available with the SAW delay lines, is that many frequencies can satisfy the conditions for CW oscillation. The resonant condition for oscillation occurs for those frequencies whose periods of oscillation are an exact sub-multiple of the total delay time around the feedback loop. As a result, the possible frequencies of oscillation form a comb spectrum with a frequency spacing between the adjacent frequencies given by $f_a = 1/\tau_a$, where τ_a is the total delay time. In fact, all the frequencies are harmonics of f_a. Since the SAW transducers of the delay line have a specific frequency response, oscillations can only occur at those frequencies which fall within the passband of the combined tranducer response. In general, only that frequency for which the initial loop gain is maximum will be excited; however, under certain conditions mode jumping to nearby frequencies can occur which results in unstable multifrequency operation.

The Mode Locked SAW Oscillator utilizes the multiple frequency operation capability of such oscillators to its advantage. In the MLSO oscillator a set of signals is excited in the comb spectrum of possible CW signals as limited by the circuit bandwidth. If specific amplitude and phase relationships are maintained between the harmonically related components of the output spectrum, the SAW oscillator can operate as a regenerative pulse oscillator because of the constructive and destructive interference of the integrally related frequencies. Since the SAW delay time determines the pulse repetition rate as well as the existing rf frequency components, the rf components in the output spectrum are all harmonics of the pulse repetition frequency. The operation of a SAW oscillator as a pulsed oscillator can be understood by considering the start-up of an oscillator using a SAW delay line. If a short burst of energy within the passband of the transducers is introduced into

the loop, it will be amplified and it will continue to circulate if the loop gain initially exceeds the circuit losses. However, because of the frequency selective nature of the circuit, there will be a tendency for this pulse to become less and less well defined as it circulates around the loop. Finally, a state of stable, single frequency, CW operation will be reached with the amplifier approaching a state of saturation such that the net loop gain is unity. On the other hand, if an element could be introduced which continues to sharpen the pulse as it circulates around the closed loop, then the pulse mode of operation could be made to persist.

The pulsed mode of operation can be accomplished by using an amplitude expander circuit, as was done by Cutler (Ref. 5), together with the conventional SAW delay line oscillator as is indicated in Fig. 3.1. The signal expander action in the circuits investigated under this program was provided by the nonlinear characteristics of a semiconductor diode. The expander is shown in general form in Fig. 3.1. At small signal levels the diode provides linear operation, but with high insertion loss for the expander. However; above a certain input threshold level where the diode impedance changes, the expander insertion loss decreases rapidly. By this tendency of the diode, the expander attenuates the lower amplitude portion of the pulse more than the higher amplitudes; thus the expander sharpens the pulse. The correct phase and amplitude conditions for the harmonically related components are established by the stability and coherence of the circulating pulse. The number of harmonically related components will be restricted to those within the passband of the circuit. The passband of the loop provides a limit on the minimum pulse width the MLSO can generate. It is desirable to have the ~~low~~ level insertion loss of the expander such that the oscillations can initially start. Lacking this, a synchronizing trigger pulse can be used to activate the expander so that a pulsed signal can begin circulating around the loop at a level high enough to remain self-sustaining.

3.2 Expanders

Several expander circuits using semiconductor diodes were evaluated during the course of this program for optimum performance and for the possibility of self starting in the MLSO mode of operation. The most satisfactory operation and the most rapid change in output with input signal level (i.e., good signal level expansion), was obtained with the circuit utilizing a transformer shown in Fig. 3.2. In this circuit, the voltage between the center tap of the transformer and the diode-capacitor arms function can be made very small at small signal levels corresponding to a high insertion loss. The circuit balancing is done with capacitors C_1 and C_2. The circuit functions essentially as a bridge. For large signals the diode impedance changes greatly with the result that a relatively low insertion loss is obtained. The circuit in Fig. 3.2 also includes provisions for applying a dc bias and a trigger signal. The expander circuit shown in Fig. 3.3 is a simpler circuit using only the voltage-divider action between the amplitude dependent diode impedance and the combined impedance of the SAW transducer and the bias and trigger line impedances.

The expander action for this circuit was not quite as good as that using the transformer, both in terms of amplitude response and its ability to sustain mode locked oscillation in the absence of a trigger signal.

The amplitude responses of the transformer type expanders used in the final apparatus are given in Fig. 3.4. Nominally a 5 dB input change from the threshold power levels gives approximately a 15 dB output change. For comparison, Fig. 3.5 shows measurements on the voltage divider type of expander. The results in Figs. 3.4 and 3.5 are similar. The diodes used in these expanders were the HP 2811. The best operating results for the expanders incorporated into the MLSO were obtained with essentially zero bias on the diodes; although, both the threshold level for expansion and small signal attenuation could be varied with the bias level. Figure 3.6 shows an extremely good response with an HB 3039 diode; however, the threshold power for expander action was too large for the amplifiers used in the mode locked loop. Proper action of the expander and oscillator requires that the amplifiers in the loop begin to saturate as the expander begins to narrow the pulse width.

The criterion for satisfactory operation of the expander was that self mode locking operation could be initiated and that the pulsed operation would continue both with and without the trigger signal present. Under these conditions, a narrow pulse width consistent with the circuit bandwidth was obtained. An excessive amplitude in the trigger signals would tend to hold the expander in the low loss state and result in widening the circulating pulse.

A simple direct technique for reliable self starting was not devised. Instead, for the purposes of demonstrating the frequency synthesis technique, trigger pulses from a video pulser were used to synchronize both MLSO and also to ensure self starting.

The expander circuit with the diodes mentioned above essentially followed the instantaneous rf voltages as illustrated by the photographs of the output waveforms in Fig. 3.7. The waveforms show a half-wave rectifier characteristic under large signal operation at $f_1 \sim 60$ MHz and $f_2 \sim 85$ MHz. The expander action can be recognized by comparing the relative peak to peak amplitudes under large signal conditions to those at small signal conditions. The large signal expander loss, because of the half wave rectification, includes 6 dB of intrinsic loss. The fast response of the expander is required in order to maintain the narrow pulsed widths desired for driving the CZT sections.

The expander bias levels provided variable attenuation in the feedback loop of the SAW oscillator as well as expander threshold voltage control. However, the zero bias condition generally resulted in the best waveforms and so most of the results were obtained with zero dc voltage applied to the bias terminals.

The characteristics of the expander were also influenced by the input impedance of the SAW transducers of the delay line and by those of the bias and trigger circuits. However, the transformer type of expander tended to be less dependent upon load conditions. For reference purposes, the frequency response and input impedance of the two MLSO delay lines are shown in Fig. 3.8 and 3.9. The high level of transducer input impedance certainly requires that the expander circuit of Fig. 3.3 must use additional shunt impedances of the order of 50 ohms to achieve satisfactory operation. The curves in Fig. 3.5 show that the most satisfactory results were obtained with 33 ohms.

3.3 MLSO Experimental Results

Two Mode Locked SAW Oscillators were fabricated for the CZT frequency synthesizer since two counter-flowing chirped signals were required at different frequencies. The rf pulses from the two MLSO's however, must be synchronized and stable. The MLSO's were fabricated according to the circuits of Fig. 3-1 and Fig. 3.2 that were discussed earlier in Section 3.1 and 3.2.

The self mode locking form of operation was obtained by either triggering the expander, to start the circulating rf pulses, or by initially increasing the loop gain by means of the amplifier bias to start CW operation. From the CW operation, the change to pulsed operation was obtained by carefully reducing the loop gain. Once pulsed operation was initiated by either technique, the loop gain could be varied within limits to increase the pulse amplitude. With the correct choice of adjustments and components, the circulating pulse is stable and will have a narrow pulse width dictated by the bandwidth of the combined SAW transducer response. Generally, excessive trigger signal level or excessive loop gain causes the pulse width to increase beyond the minimum value. In the first case, the expander does not turn off soon enough and in the second case, the amplifier saturation counteracts the expander.

The triggered mode of operation was selected as the most practical one for this program. The same trigger signal applied to the two MLSO's brings about the desired synchronization of the two pulses. A more complex arrangement, which would involve one self mode locked oscillator providing a trigger for the second, was set aside. In the triggered mode it was possible to establish a trigger level and loop gain level which permitted the two MLSO's to start instantly with the desired pulse shape. However, excessive trigger levels would cause the pulses to widen.

The quality of the two output signals after the circuits were adjusted is shown in Fig. 3.10. The pulse-to-pulse coherence is demonstrated by the stable rf waveforms obtained on an externally triggered oscilloscope (see Fig. 3.10). In taking these oscilloscope records of the signals waveforms, the sweep was initiated by the trigger signals to the expander, thus also indicating that the pulse repetition

frequency and the rf frequencies were harmonically related. The frequencies indicated in Fig. 3.10 are only approximate since they were determined from the time calibration of oscilloscope sweep. The signal frequency f_1 is the 74.5 harmonic and f_2 is the 101.5 harmonic of the pulse repetition frequency of the MLSO's. The half harmonic values correspond to the amplifier chains being inverting. The synchronized waveforms of Fig. 3.10 were only obtained after it was recognized that there were unequal delay times in the two oscillator loops and a correction was made. A short section of coaxial line (delay time of 20 ns) was added to the loop at f_2 to conpensate for the fact that the loop for f_1 had an additional tuning inductor. With the delay times matched, both MLSO's could be simultaneously locked to a common synchronizing signal. An example where the delay times were not perfectly matched is indicated by Fig. 3.11a where the trigger repetition frequency was such that only f_2 remains locked to the trigger. In Fig. 3.11b are seen waveforms where both signals are unlocked. Unlocked means that the rf frequency was not harmonically related to the synchronizing frequency and therefore the individual rf cycles are not fixed within the pulse envelope. A set of oscilloscope records of a synchronized MLSO including the output power spectrum is shown in Fig. 3.12. The level of spurious signals between comb lines is well below 60 dB and the full spectrum replicates the transducer response. The results in Fig. 3.12 are not those for the final delay line but are typical of what can be obtained.

4.0 EXPERIMENTAL RESULTS WITH THE CZT FREQUENCY SYNTHESIZER

4.1 Description of the Apparatus

The apparatus for studying a frequency synthesizer using CZT transducers and programmable nonlinear taps was used in several different type experiments in order to get an understanding of how various parameters effect the operation. This section includes the results of three different experiments; they are: 1) frequency synthesis with pulsed variable frequency carriers and CZT waveforms, 2) frequency synthesis with MLSO pulses and CZT waveform and, 3) frequency synthesis with short continuously chirped pulses.

The full apparatus for using the two MLSO's and CZT SAW devices is shown by the block diagram of Fig. 4-1. Originally, it was planned to fabricate all of the SAW components, the two MLSO delay lines, the two sets of CZT transducers, the tap array and the SOS diode array on one piece of $LiNbO_3$. However, subsequent experiments indicated that the stray radiation from the strongly amplified signals applied to the CZT, interferred with the MLSO oscillators. As a result, the final assembled apparatus contained two complete sets of SAW components, one containing only the two MLSO's and the other the two CZT's, the taps and the diode array. In the block diagram these SAW devices are denoted as M239 and M238, respectively. All MLSO loops contain a SAW delay line, an expander, a resistive signal coupler, and two broadband amplifiers. Amplifier A_1 is an Avantek VTO51 and VTO511 and Amplifier A_2 is an Avantek VTO513. Amplifier A_1 is provided with variable voltage for controlling its gain. Amplifier A_2 is capable of delivering approximately 30 milliwatts. The amplifiers designated as A_3 are separate external amplifiers that were added because it was found necessary to increase the pulse amplitude delivered to the CZT's in order to increase the signal to noise ratio at the output of the synthesizer. The seventeen control switches are manual SPST switches that can connect the "ON" bias supply to any of the diodes as desired. The Sync generator provides a common trigger signal to the two expanders. An external high pass filter allows just the programmable sum frequency signal to be extracted. Not shown in the block diagram is a mixer and local oscillator (at nominally 140 MHz) that generates a base band signal. Easily recognizable programmable sinusoidal signals are seen only at base band with this frequency synthesis technique.

A photograph of the assembled apparatus is shown in Fig. 4-2. The photograph has additional details not given in the block diagram of Fig. 4-1. These additional details include the controls for the bias for each of the amplifiers designated as A_1, the "ON" bus and controls for its bias, and the separate terminals or ports for the CZT's and MLSO outputs.

The various bias levels are: amplifiers type A_1, require +15 volts, amplifiers type A_2 require +24 volts, the "ON" bus requires a variable supply up to about 3 volt (one diode draws about 0.05 ma for maximum nonlinear output.)

The SAW components of the CZT frequency synthesizer are shown in the photograph of Fig. 4-3. The delay lines at f_1 and f_2 for the MLSO's are seen as two parallel paths. The long CZT transducers are each a pair of parallel transducers with $\sin x^2$ and $\cos x^2$ weighting and with a $\pi/2$ radian off-set. The output sine and cosine signals from the two parallel transducers are actually added at the taps which are long enough to intercept both signals. Wire bonds are used for connections to various bonding pads on the $LiNbO_3$ and for connections to the diode array. The important time dimensions for the CZT transducers and the tap region are given in Fig. 4-4. The 16 finger sets in the CZT transducers are spaced 76.5 ns apart and the 17 finger sets in the tap region are 38.1 ns apart. The dimensions will be useful in interpreting the experimental waveforms. The finger pairs in the CZT are further split into 1/8 wavelengths widths to reduce finger reflections.

The diode array using Silicon on Sapphire fabrication is shown magnified in Fig. 4-5. The mode array was fabricated in our own facilities. The diodes are spaced by 5 mils and are connected to a common output bus. The diode array was bonded to the base plate along side the SAW components. The "ON" state consists of biasing a diode for optimum efficiency in mixing. This corresponds to a diode current less than 0.1 ma. At zero bias current, the diodes are left floating. The signal levels on the output bus were 15 to 20 dB less than the desired signal generated by mixing. A diode could also be switched into a linear mode, at about 0.8 ma, for which no significant mixing occurs; for this condition, the sum of the two SAW signals is obtained. This mode of operation was useful for signal diagnostics. The element values in the diodes in the array are; bias resistor - 2500 ohms, diode capacitance at "0" bias - 1 pf, and an equivalent series resistance of 50 ohms.

4.2 Observations of Waveforms with Pulsed rf Signals

The CZT section of the frequency synthesizer was evaluated by driving the transducers with short rf pulses that were generated by applying switching techniques to cw signals. In this way the rf frequencies and pulse repetition frequencies could be used as parameters in the experiment. In addition, the cw sources could also be used to generate a synchronized L.O. signal that, in turn, could be used to produce the base band signal from the synthesized signal. The block diagram of the experimental set-up is shown in Fig. 4-6. The higher frequency f_2 (nominally 85 MHz) and the sum frequency f_3 (nominally 142 MHz) are generated by tunable cw oscillators. The lower frequency f_1 is generated from f_2 and f_3 by mixing (i.e., $f_1 = f_3 - f_2$). Thus the synthesized signal at the sum carrier frequency

is always synchronized with the sum frequency L.O. signal. This fixed phasing between the two signals results in a stabilized output signal at base band. High pass and low pass filters were used, where required, to remove unwanted signals (refer to Fig. 4-6). The experimental parameters included f_2, $f_3 = f_1 + f_2$, pulse repetition frequency and tap selection for nonlinear operation or linear operation. The signal levels of the pulsed rf at the CZT transducers could be made as large as 30 dBm.

Typical signals from the CZT transducers as they appeared at the taps are displayed in Fig. 4-7. Both single bursts to show spurious signal levels, and contiguous bursts to show the continuous signal are included. The timing between single chips, the timing between the input pulse and the CZT bursts, and the pulse lengths are in agreement with the timing diagram in Fig. 4-4. The accuracy of the relative timing between the two counter flowing bursts is indicated by the signals in Fig. 4-8. Here the diodes are set for linear switching so that the two signals simply add or more correctly overlap, since the carrier frequencies are different. With a length of approximately 50 ns, the individual chips from the two signals are seen to overlap very accurately and the beginning of each CZT burst at a tap is pronounced. The results shown in Fig. 4-8 have raised one unresolved question, however. According to the physical dimensions of the original art work, the dimensions of the contact mask and those of the finished SAW device, the center of the tap array (tap number 9) should be exactly midway between the two CZT transducers. We have not been able to explain why the electrical signals of Fig. 4-8 indicate that tap number 11 is at the midpoint. The signals displayed in Figs. 4-7 and 4-8 show that the amplitudes of the individual chips are only reasonably constant. This is indicative of the uniformity of the array of fingers and also of the accuracy of the amplitude weighting. The correlation of a discrete chirp signal is shown in Fig. 4-9 where all of the taps are simultaneously turned on in the linear switching mode. The correlation peaks appear with a periodicity in carrier frequency of approximately 0.8 MHz which is the chip frequency. The frequencies for which the correlation peaks are found are accurate; however, some personal judgment was involved in determining when the "best" correlation occurs. This accounts for why the frequency differences are not in more accurate agreement.

The frequency synthesis with the pulsed rf signals driving the CZT transducers resulted in the signal wave forms shown in Figs. 4-10 and 4-11. To obtain these results, all the variables listed earlier were adjusted for the best base-band wave forms. The signals recorded in these figures include those from all of the operating taps. After final assembly of the SAW components, it was found that taps numbered 1, 2, 8, and 10 were not operating. The set of frequencies which gave the results were: $f_1 = 60.5$ MHz, $f_2 = 85.5$ MHz, and a repetition frequency of 0.834 MHz. The design frequencies were: $f_1 = 5.72$, $f_2 = 85.8$, and 0.827 MHz (these values are based upon the physical length of the CZT transducers). For the results in Fig. 4-10, the frequencies were adjusted to give zero frequency at tap 9, the physical center

of the tap array. For Fig. 4-11, f_1 was reduced so that the zero frequency signal appeared at tap 17. The general quality of the sinusoidal signals leaves room for improvement and, in part, is due to leakage through the turned-off switches, electromagnetic coupling, lack of uniformity in the CZT transducers, and inadequate filtering.

An unanticipated result was the capability of the base-band zero frequency position to be shifted at will from one end of the tap array to the other by shifting one of the pulse carrier frequencies. Recall that the base-band signal was generated by providing a local oscillator signal at exactly the sum frequency of the two pulsed carrier frequencies. The explanation is obtained from the analysis in Section 2.3 which showed that the effective carrier frequency for the SAW signals generated by the CZT transducers is independent of the input pulse carrier frequency; it is only determined by the spacing between the finger sets of this transducer. Therefore, if the rf carrier frequencies are varied in the experimental set up of Fig. 4-6, the net effect is as though only the local oscillator frequency were varied. For this reason, the zero frequency base band signal can be positioned at any one of the taps. For a carrier input frequency that places the zero frequency at an intermediate position between taps no recognizable base band frequency is obtained. In fact, it was found that the input frequencies must be set within approximately $\pm$ 20 KHz of the correct frequencies in order to obtain good base-band signals. One question raised by these experiments is whether or not the synthesized sum frequency signal may in fact be a good quality signal over a wider range of carrier frequencies than the experimental technique of Fig. 4-6 indicates.

The physical dimensions of the SAW device give a 76.5 ns spacing between finger sets in the CZT. This yields a chip frequency or sample frequency of 13.07 MHz. Based upon this fact, the operating frequencies should be 65.36 and 91.5 MHz. For a chip frequency of 12 MHz, the operating frequencies should be 60 and 84 MHz. These small but perhaps significant discrepancies may partially explain why better waveforms and wider ranges in input signal frequencies were not found.

An estimate was made of the period of the continuous frequencies generated from the oscilloscope time calibration of Figs. 4-10 and 4-11. The values determined compare favorably with the table of values (Table 4-1) based upon harmonics of the lowest frequency possible namely $1/T = 0.833$ MHz (where $T = 1.2$ µs, the chirped pulse length was determined from the oscilloscope traces).

TABLE 4-1

BASE BAND FREQUENCIES

Tap No.	Freq. MHz	Period μsec
1	6.664	.160
2	5.831	.170
3	4.998	.200
4	4.165	.240
5	3.332	.30
6	2.499	.40
7	1.667	.60
8	.833	1.20
9	0	∞
10	.833	1.20
11	1.667	.60
12	2.499	.40
13	3.332	.30
14	4.165	.240
15	4.998	.200
16	5.831	.170
17	6.664	.160

Chirp pulse length = 1.2 μsec
prf = 0.833 MHz

4.3 Observations of Waveforms with the MLSO's

The experiments described in Section 4.2 allowed parameters such as frequency and repetition rate to be varied so as to obtain the best possible results with the SAW components as they were designed and fabricated. The quality of the synthesized frequencies as displayed at base band, however, was not as good as desired (see Section 4.2). Similar results were obtained using the mode locked SAW oscillator to drive the CZT transducers.

The mode locked SAW oscillators fabricated in this program were essentially fix-tuned components. Provisions were not made for several iterations on SAW components fabrication in order to obtain optimum quality in the frequency synthesized signals. The apparatus used is that given in the block diagram of Fig. 3-1.

The actual operating small signal gain values were generally reduced from the maximum values possible in order to obtain good pulse waveforms. The addition of externally supplied amplifiers were found necessary in order to increase the MLSO pulsed output so that acceptable signal-to-noise ratios would be obtained at the output terminals for the programmed frequencies. The two MLSO's operated well synchronized together at 62.5 HMz and 85.4 MHz, respectively. These frequencies are not the ones found optimum for the CZT sections (see Section 4.2); however, the output signals did show partial frequency synthesis in the base band signals, see Fig. 4-12. Since the rf carrier frequencies of the pulsed signals are determined by the SAW delay lines, it was not convenient to derive a synchronized local oscillator signal at the sum frequency. Instead, a tunable oscillator was carefully tuned until an optimum appearing signal was obtained. The applied local oscillator frequency was 144 MHz. The sum frequency, determined from the calibrated oscilloscope traces of the MLSO's was 147.9 MHz. It is interesting to note than an L.O. frequency of 146 MHz and therefore a 146 MHz sum frequency was used in Section 4.2 to give a "zero beat" signal at the center tap. According to the analysis of Section 2, the physical dimensions of the CZT components determine the carrier frequency of the output signal independently of the rf pulse frequencies. Thus the fact that the center tap (Tap 9) shows a frequency of roughly 1.7 MHz instead of zero frequency is consistent with the fact that an L.O. frequency of 144 MHz is off-set by 2 MHz from the desired value of 146 MHz. The particular combination of parameters for the MLSO, where only the repetition frequency could be varied, probably explain why the synthesized waveforms were distorted.

The quality of the signals in Fig. 4-12 is critically determined by the rf carrier frequencies. This was found experimentally in Section 4.2. The analysis in Section 2 does not show this aspect of the frequency synthesizer characteristics. It is evident that in further work it would be helpful to redesign the MLSO's so that controlled changes can be made in the rf carrier frequencies in order to be able to bring all of the parameters of the SAW components into proper relationship.

4.4 Frequency Synthesis with Short-Pulsed Linear Chirps and Switching Times

The programmable output from the discrete chirps is different than that from continuous chirps. For comparison purposes, a brief experiment on frequency synthesis was carried out with continuous linear chirps within short pulses. The chirped signal was generated from a common chirp signal through a series of mixing operations. The pulse lengths were 3 microseconds. The experiment was carried out using a circuit that is equivalent to that in Fig. 4-13. The circuit was also instrumented so that electronic control signals could be applied to the diode array. In these experiments it was possible to view the output signal, in this case the difference-frequency, directly. The results are shown in Fig. 4-14a and b. In

Fig. 4-14a, signals for three different output frequencies are shown. The frequencies were estimated from the time base calibration of the oscilloscope. The quality of the sinusoidal waveforms is good and any distortion due to signal leakage from the turned-off taps is not evident on the scale of this signal display. In Fig. 4-14b switching from one frequency to another is shown; the switching is accomplished by the timing of the diode control pulses as indicated in Fig. 4-13. The switching time is seen to be less than 100 ns. Although the waveforms generated by the continuous chirps have a high quality, it must be remembered that each chirped pulse must be longer than at least twice the desired pulse length of the output in order to obtain a constant output frequency during this desired output pulse duration. The requirement for continuous pulses of different frequencies or for a cw output would require several parallel channels and a somewhat complex switching arrangement.

The purpose of this section was primarily to show the rapid switching capability of the integrated circuit diode array that was used in this program.

5.0 SUMMARY

A new type of frequency synthesizer utilizing Mode Locked SAW Oscillators, CZT transducers, and rapidly switchable nonlinear diodes was experimentally demonstrated to be both feasible and promising. The conclusions drawn from work with this first preliminary model are as follows: the Mode Locked SAW Oscillator (MLSO) is able to provide a set of synchronized and stable short rf pulses with lengths in the range of 50 to 100 ns. These pulses can efficiently drive a set of CZT transducers that are used for generating counter flowing SAW discrete chirp signals. By using the sum frequency, signals are synthesized directly at rf frequencies. The results also confirmed that the carrier frequency of the output appears to be fixed only by the CZT transducer geometry and is independent of the input pulse carrier frequencies. The programmable frequency steps are also independent of the input carrier frequencies.

The CZT components together with the programmable taps do generate programmable discrete sum frequency signals. These signals were viewed at base band in the present work since the signals at the sum frequency of 146 MHz are not easily recognized. The full range of frequencies was obtained. The quality of the base band signals, however, were found to be strongly dependent upon the relationship between the pulse carrier frequencies.

From the experimental results and the analysis it appears that the fabrication of the SAW components and exact design dimensions and other parameters will have to be more carefully controlled in order to avoid signal distortion. In further work it would be useful to modify the MLSO's so that limited tuning adjustments on the rf carrier and repetition frequencies can be made so that the output of the synthesizer can be tuned for optimum waveforms. On the practical side it would be desirable to electrically isolate the key SAW components to reduce stray signal levels and also to re-examine the way in which the components, the MLSO's the CZT's and the array of diode-tap are interconnected and coupled in order to ascertain if a stronger signal can be obtained with fewer stages of amplification.

The experiments and analysis of the results indicates that a number of problem areas exist with respect to obtaining a useful apparatus. From the promising preliminary results obtained in this program it is clear that more extensive experimental and analytical work is desired in order to determine what can be ultimately done with the MLSO-CZT frequency synthesizer in terms of signal quality, stability, range of programmable frequencies and rate of frequency hopping.

REFERENCES

1. Gilden, M., T. M. Reeder, and A. J. DeMaria: The Mode-Locked SAW Oscillator. 1975 Ultrasonics Symposium Proceedings, pp. 251.

2. Alsup, J. M., H. J. Whithouse: Frequency Synthesis Via the Discrete Chirp and Prime Sequence ROMS. Proceedings IEEE 69, pp. 721-723, May 1976.

3. Kroupa, V.: Frequency Synthesis. Halsted Press/John Wiley, New York, 1973.

4. Reeder, T. M., T. W. Grudkowski: Programmable PSK Diode Convolver. Electronics Letters 12, pp. 186-187, April 1976.

5. Cutler, C. C.: The Regenerative Pulse Generator. Proc. IRE, February 1955, pp. 140-148.

6. Hargrove, L. W., R. L. Fork, and M. A. Pollack: Locking of He-Ne Laser Modes Introduced by Synchronous Intracavity Modulation. Appl. Phys. Letters 5, 1964, pp. 4-5.

7. DeMaria, A. J., D. A. Stetser, and W. H. Glenn, Jr.: Ultrashort Light Pulses. Science 156, June 23, 1967, p. 1557-1568.

8. Lewis, M. F.: Some Aspects of SAW Oscillators. Ultrasonics Symposium Proceedings, 1973, pp. 344-347.

MODEL FOR COUNTER FLOWING DISCRETE CHIRPS

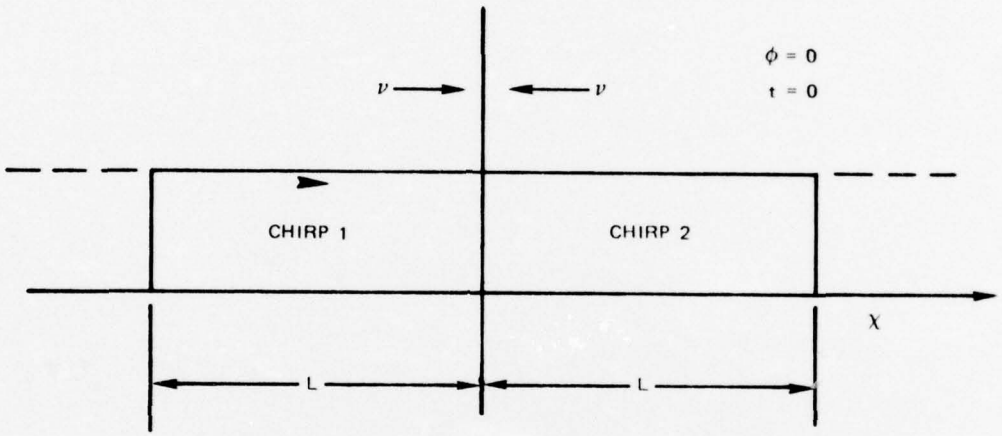

a) INITIAL POSITIONS OF SIGNALS

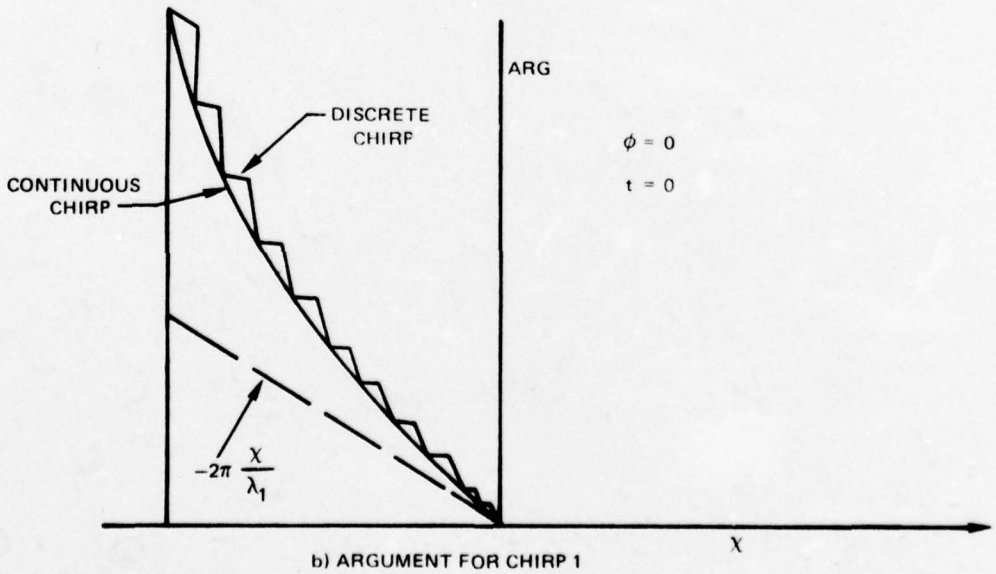

b) ARGUMENT FOR CHIRP 1

FIG. 2-2

FREQUENCY SYNTHESIS TECHNIQUE

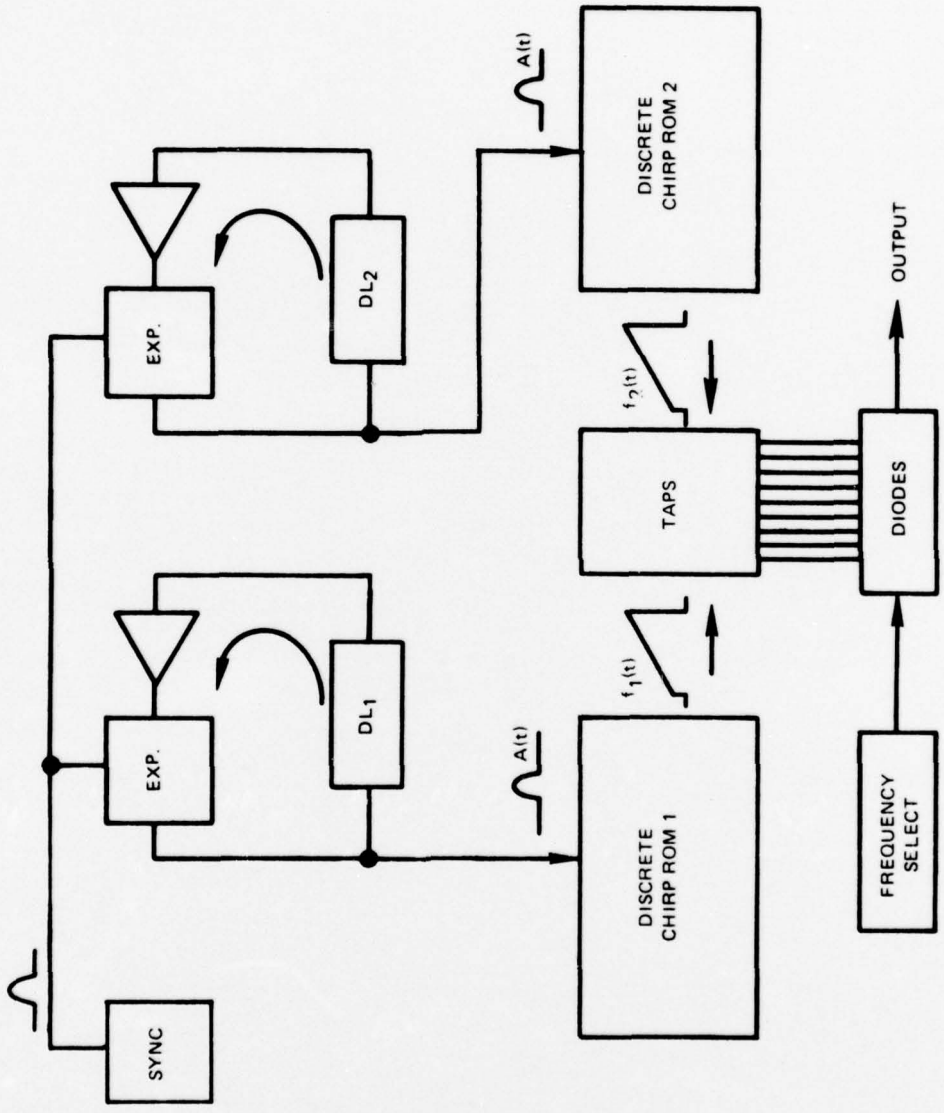

R12-27-1

FIG. 3-1

FUNCTIONAL CIRCUIT DIAGRAM OF MLSO

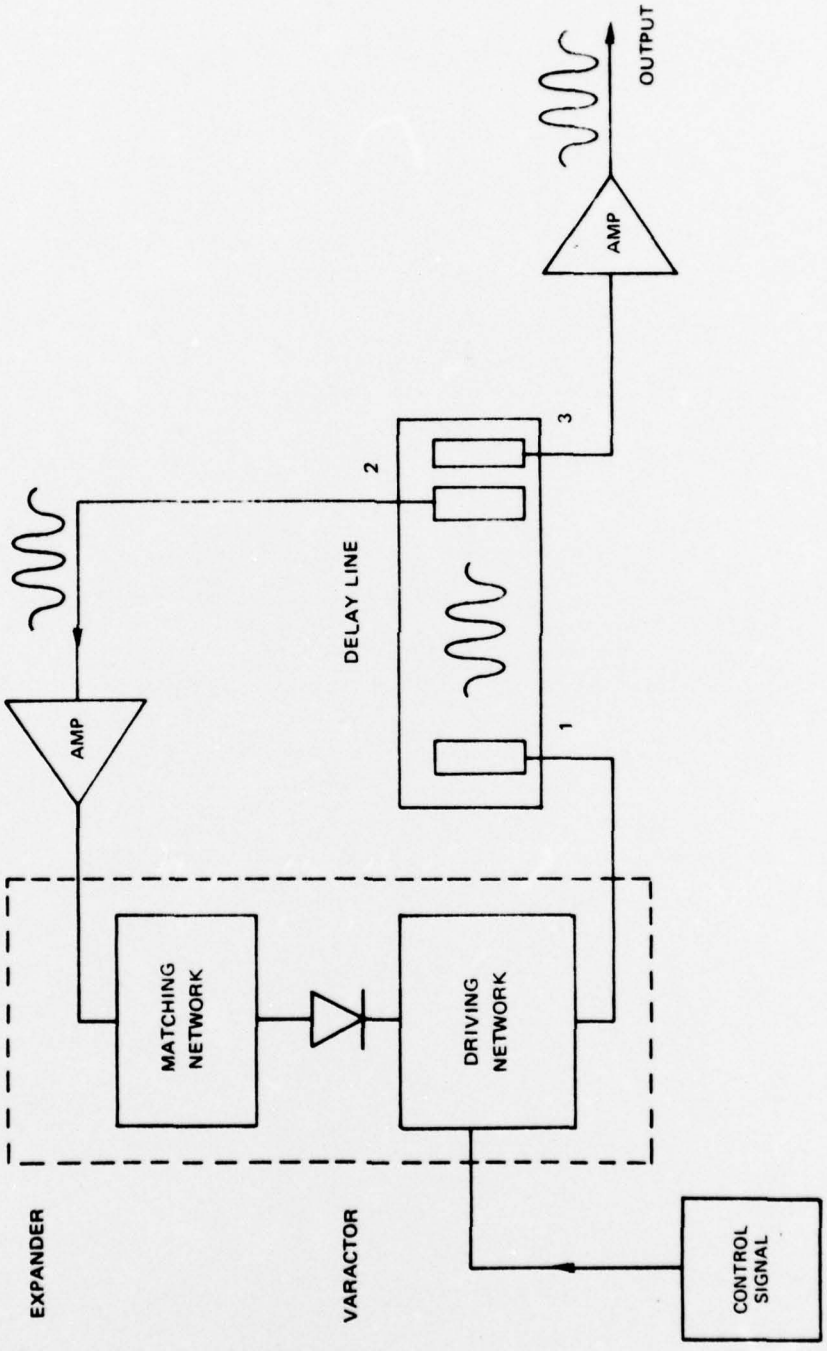

76-02-86-1

FIG. 3–2

CIRCUIT DIAGRAM OF EXPANDER UTILIZING TRANSFORMER

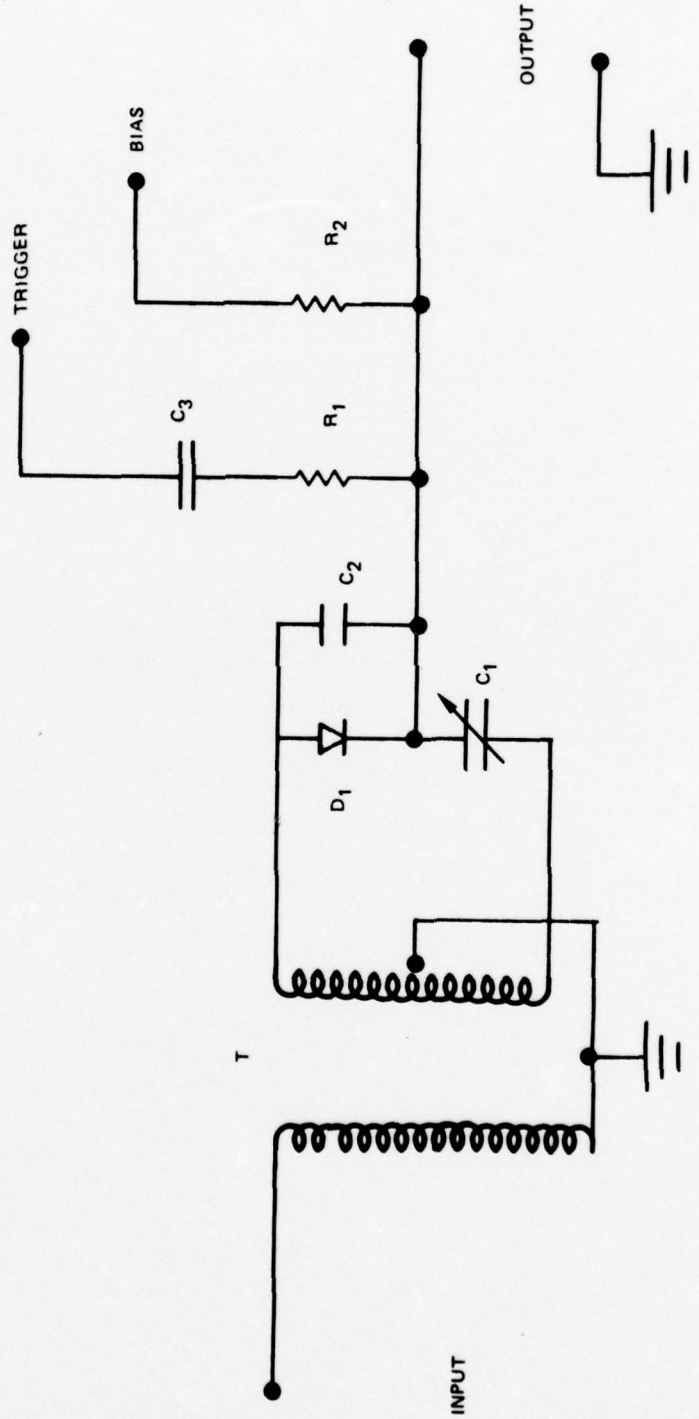

76–08–106–8

FIG. 3-3

CIRCUIT DIAGRAM OF EXPANDER UTILIZING VOLTAGE DIVIDER

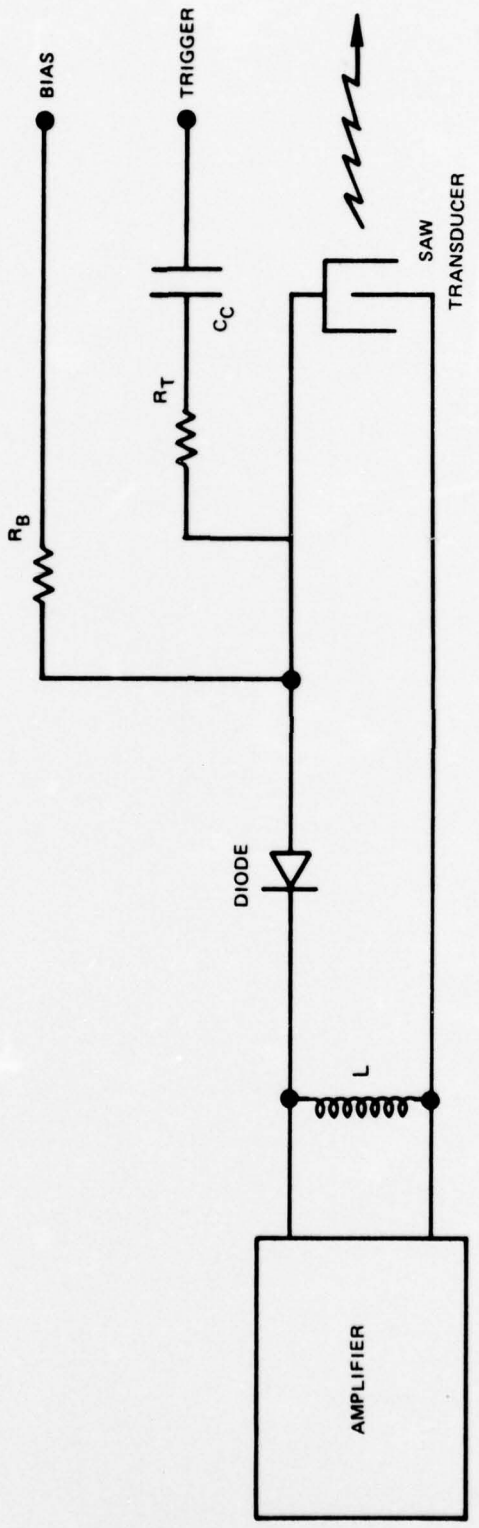

76-08-178-5

FIG. 3–4

EXPANDER AMPLITUDE RESPONSE

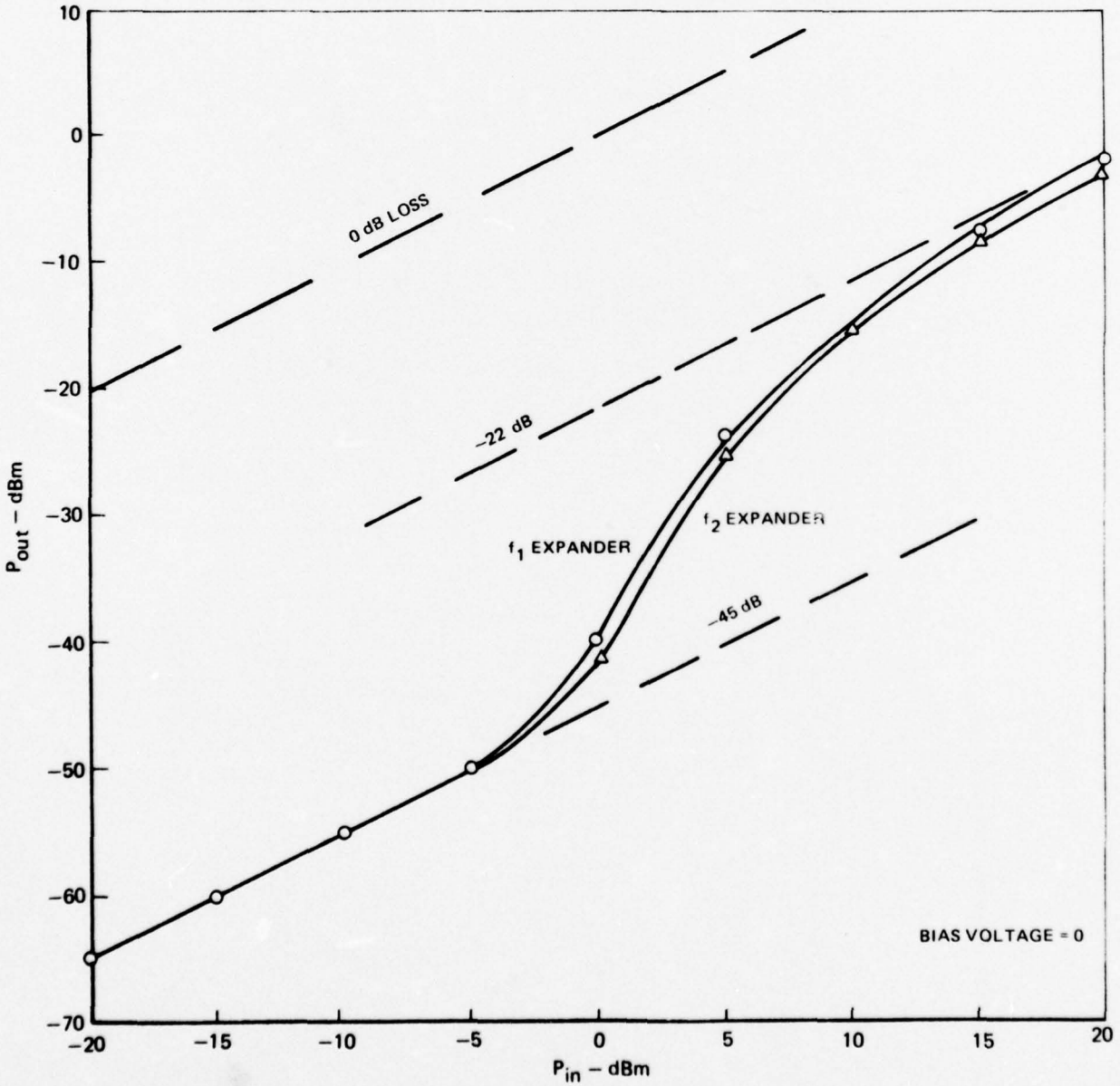

76–08–126–2

EXPANDER WITH HP 2811 DIODE

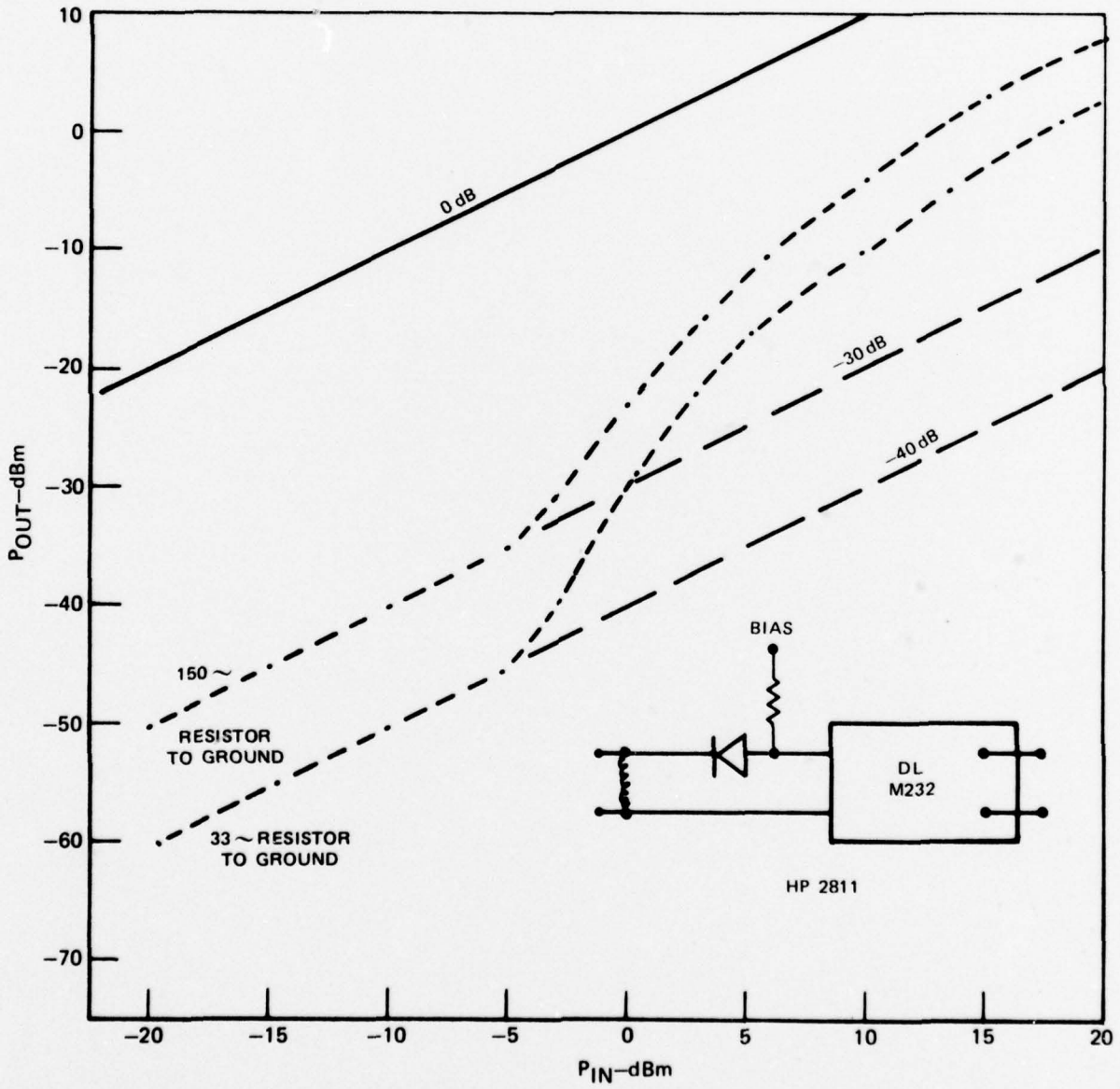

76–08–194–2

FIG. 3–6

EXPANDER WITH HP 3039 DIODE

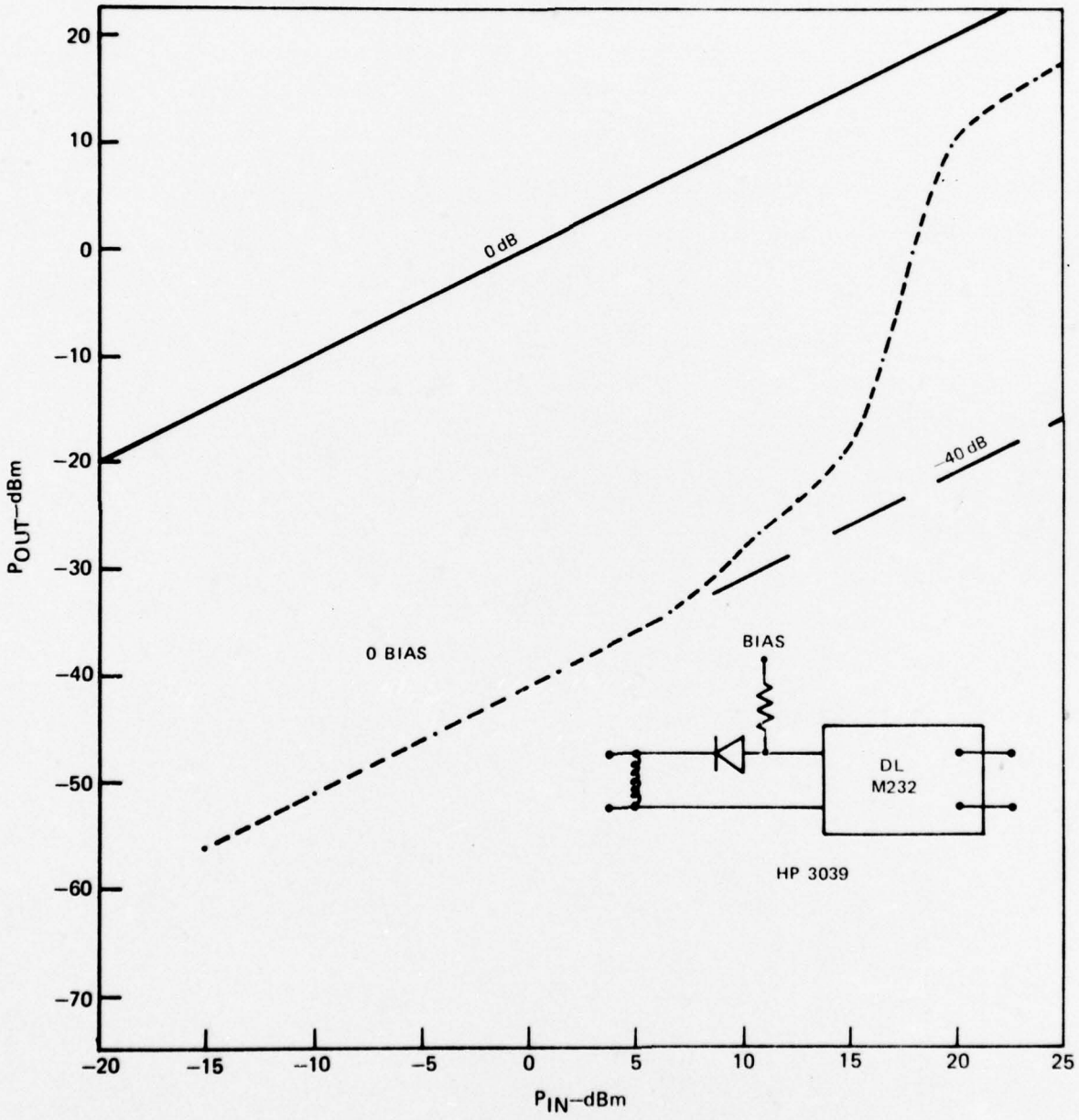

76–08–194–3

FIG. 3–7

EXPANDER WAVEFORMS

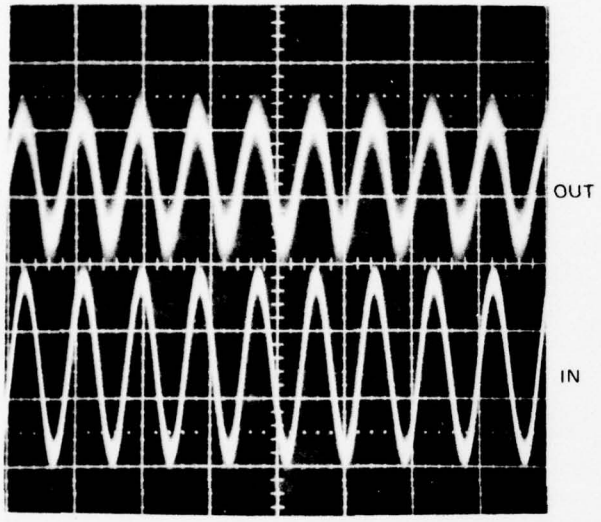

a) OUT – 10 mV/DIV
IN – 0.1 V/DIV
THRESHOLD, f_1

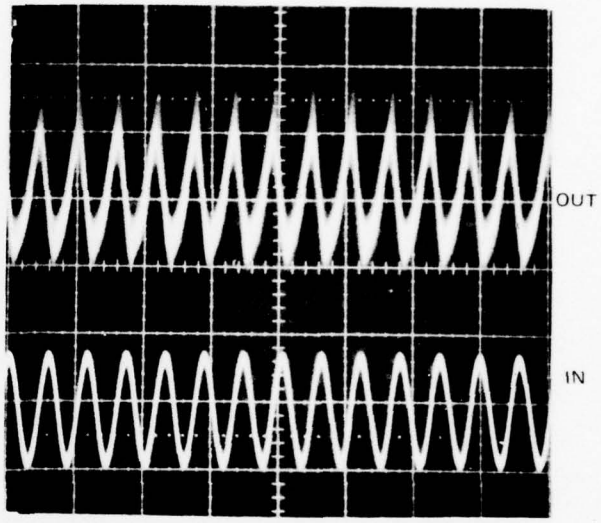

c) OUT – 10 mV/DIV
IN – 0.5 V/DIV
THRESHOLD, f_2

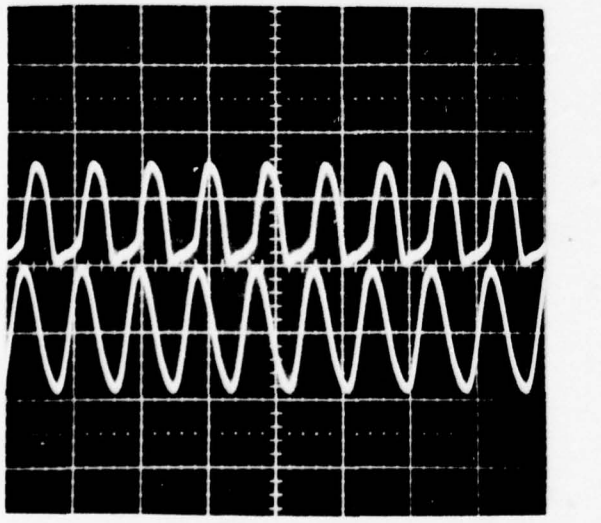

b) OUT – 0.5 V/DIV
IN – 1 V/DIV
AMPLIFIER SATURATION, f_1

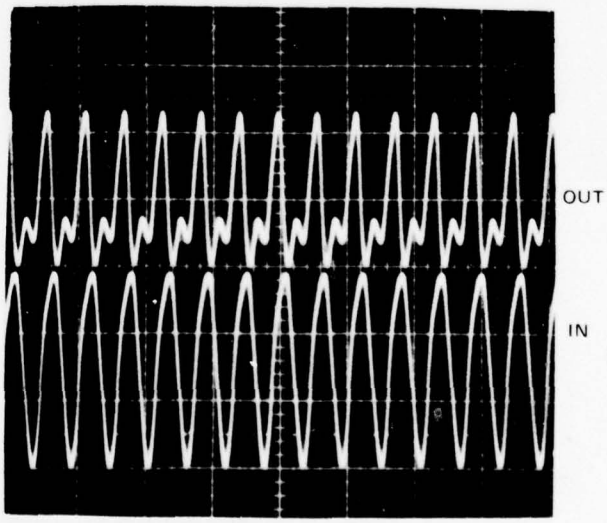

d) OUT – 0.2 V/DIV
IN – 1 V/DIV
AMPLIFIER SATURATION, f_2

FIG. 3-8

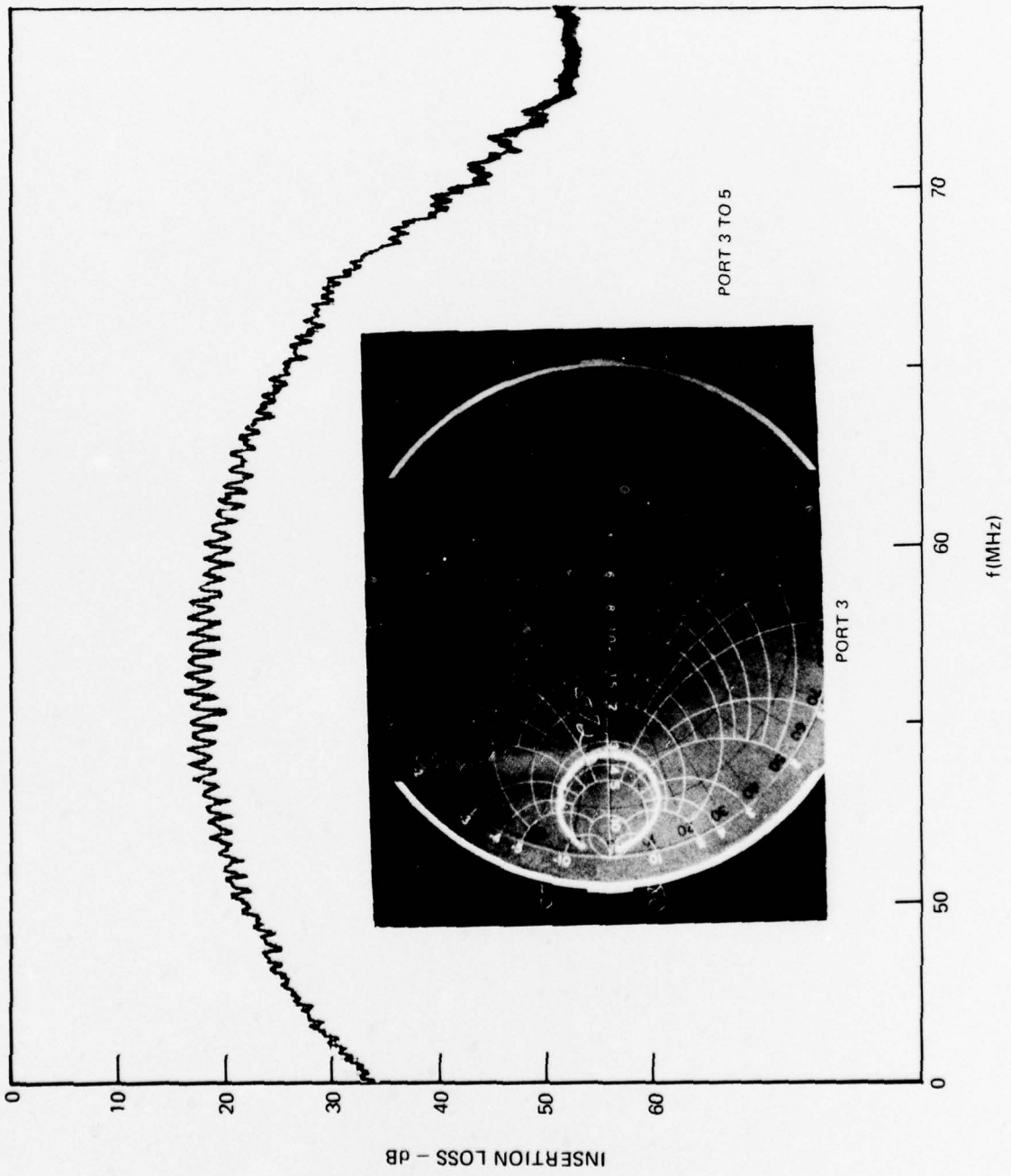

76-08-178-4

FIG. 3-9

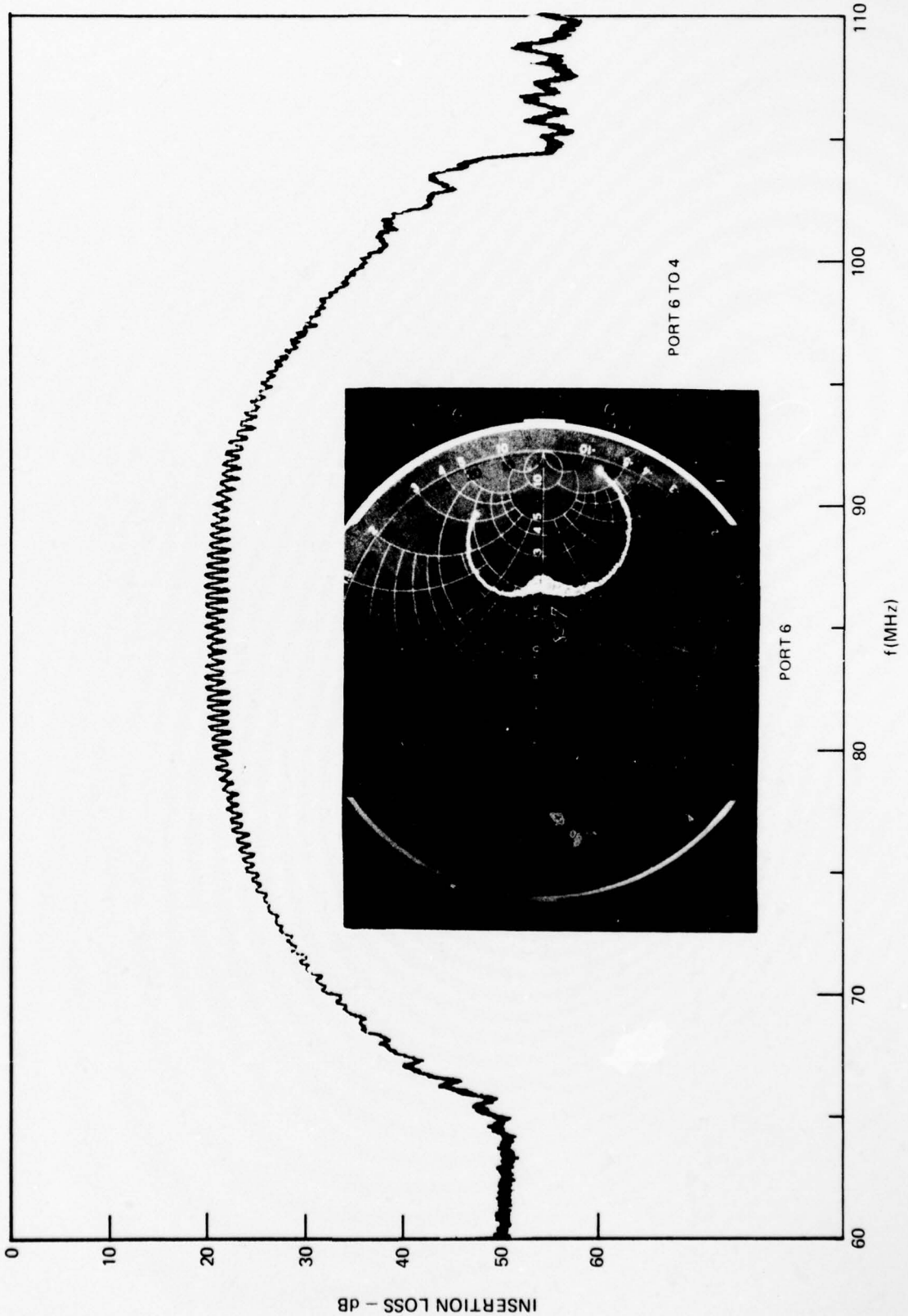
DELAY LINE FREQUENCY RESPONSE FOR f_2
INSERTION LOSS – dB
0
10
20
30
40
50
60
f(MHz)
60
70
80
90
100
110
PORT 6
PORT 6 TO 4
76-08-178-3

FIG. 3–10

MLSO SYNCHRONIZED PULSED OUTPUTS

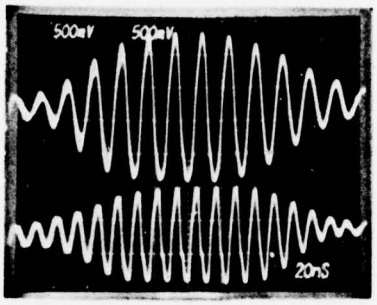

$f_1 \sim 62.5$ MHz

$f_2 \sim 85.4$ MHz

a) SYNC PRF = 0.840
SWEEP SYNCHRONIZED TO
SYNC SIGNAL

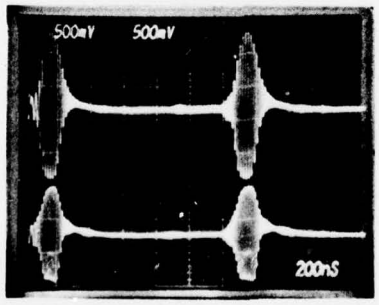

f_1

f_2

b) PRF = 0.840 MHz

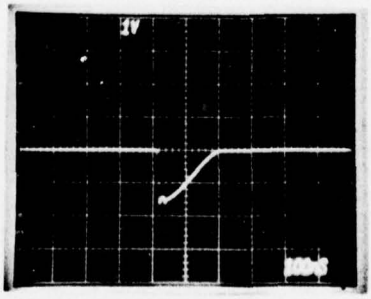

c) SYNC SIGNAL APPLIED
TO EXPANDERS

76–08–106–1

FIG. 3–11

MLSO PULSED OUTPUT NEAR SYNCHRONIZATION

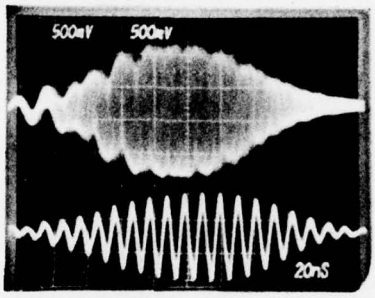

f_1 –

f_2 = 93.75 MHZ

a) SYNC PRF = 0.837 MHz
SWEEP SYNCHRONIZED
TO SYNC SIGNAL

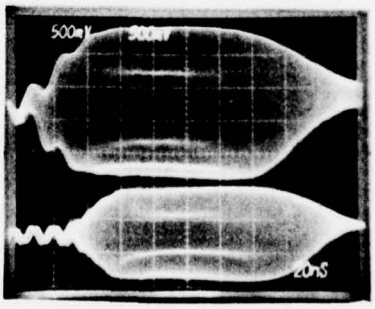

f_1 –

f_2 –

b) SYNC PRF = 0.828
SWEEP SYNCHRONIZED
TO SYNC SIGNAL

MLSO SIGNAL CHARACTERISTICS WITH LOCKING PULSE

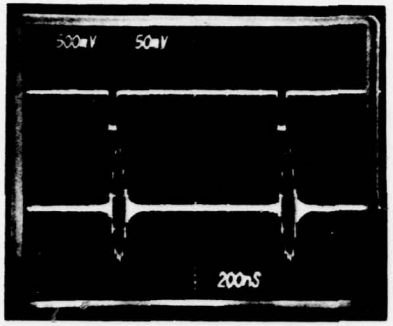

LOCKING PULSE

SYNCHRONIZED RF PULSE

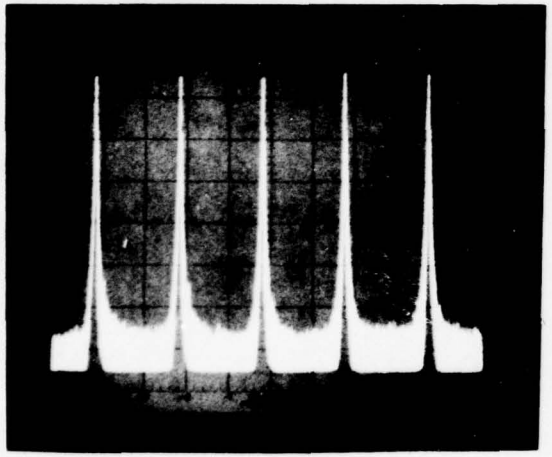

b) SPECTRAL LINES (0.5 MHz/DIV, 10 dB/DIV.)

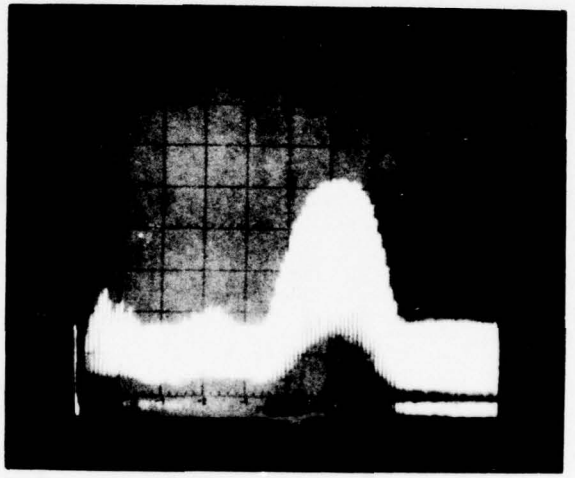

d FULL SPECTRUM (0–100 MHz, 10dB/DIV.)

FIG. 4–1

BLOCK DIAGRAM MLSO CZT FREQUENCY SYNTHESIZER

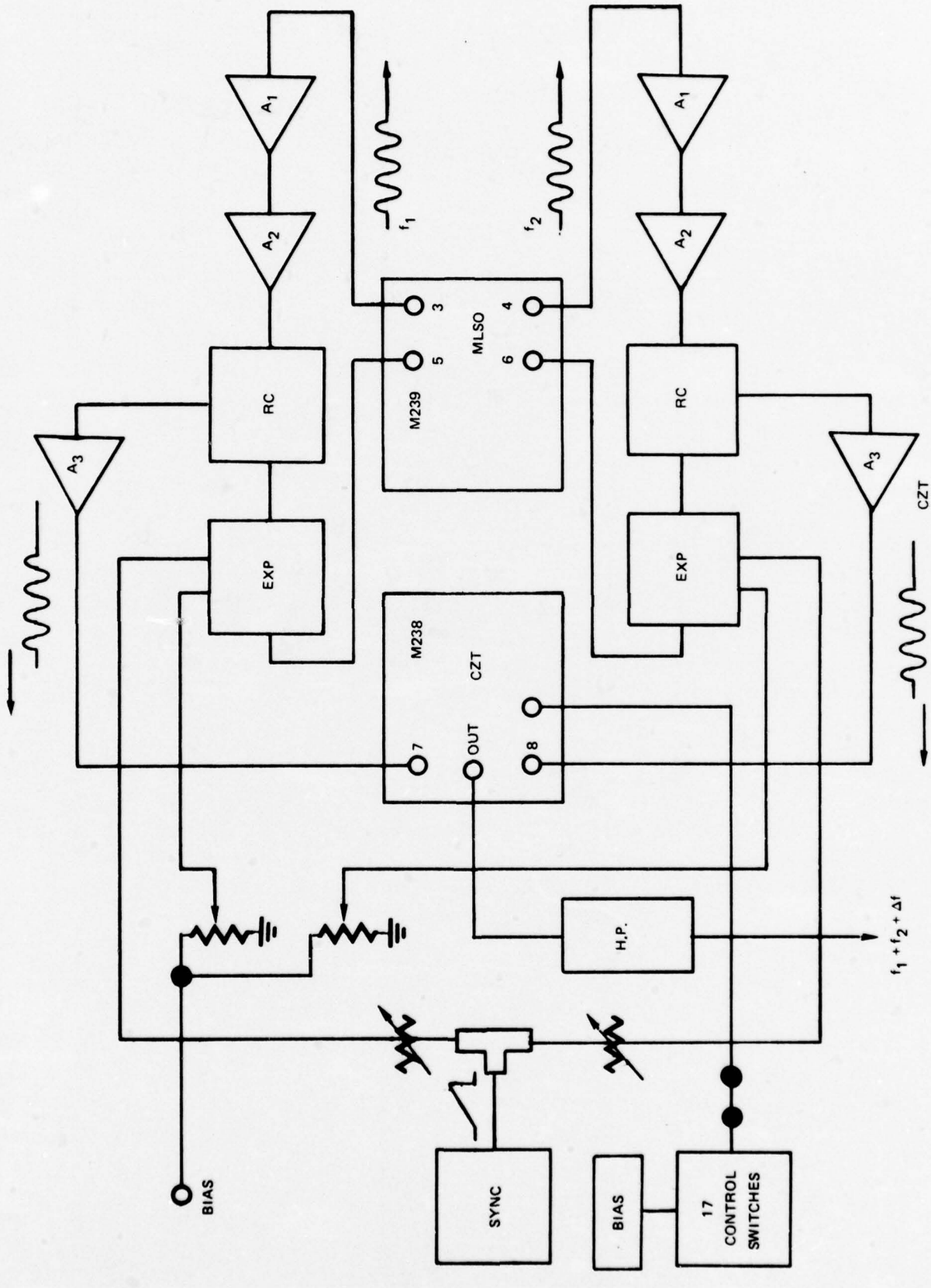

76–08–106–3

PHOTOGRAPH OF APPARATUS

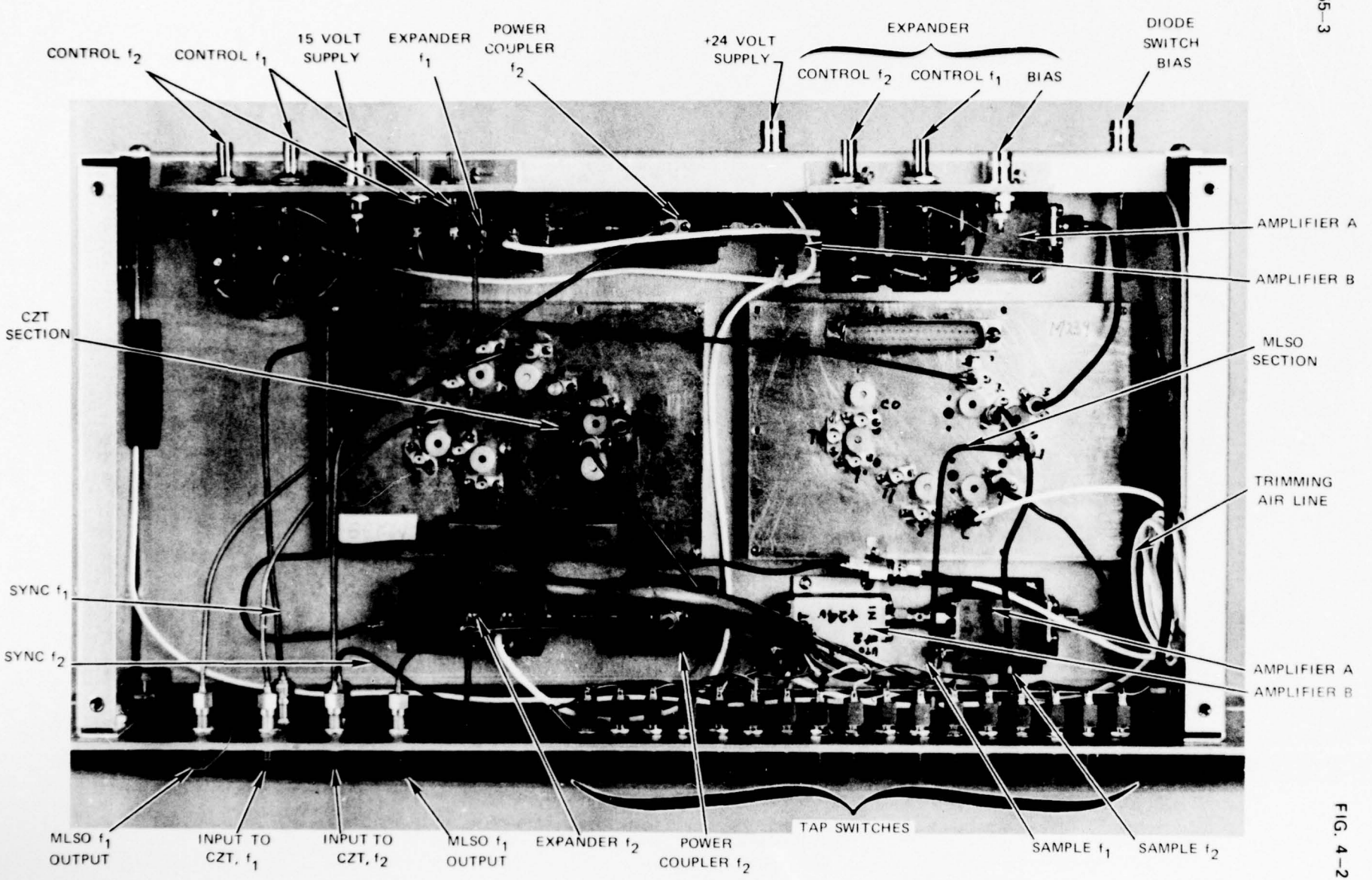

R76-922155-3

FIG. 4-2

PHOTOGRAPH OF SAW COMPONENTS AND DIODE ARRAY

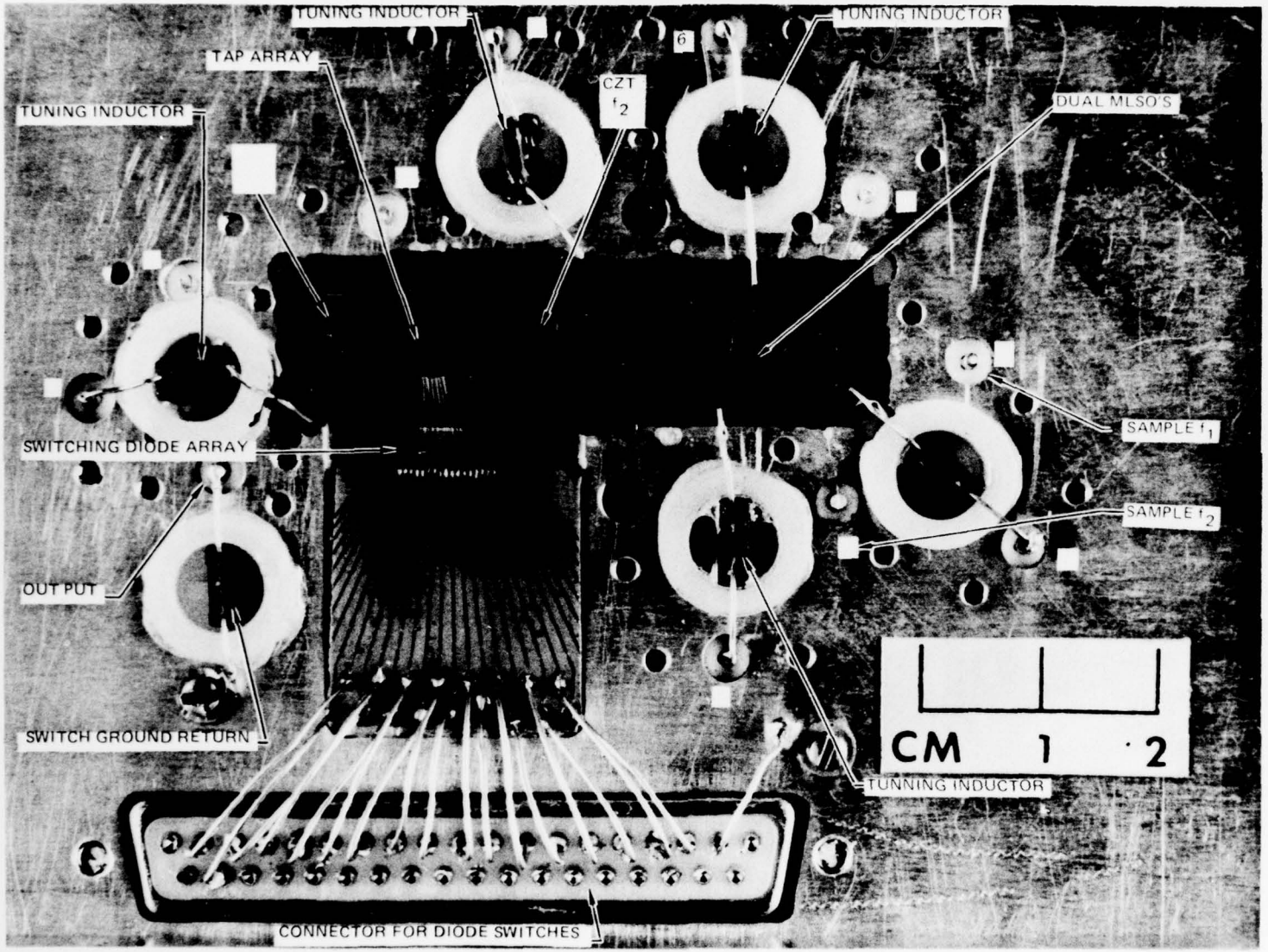

R76-922155-3

FIG. 4-3

76-08-126-1

FIG. 4-4

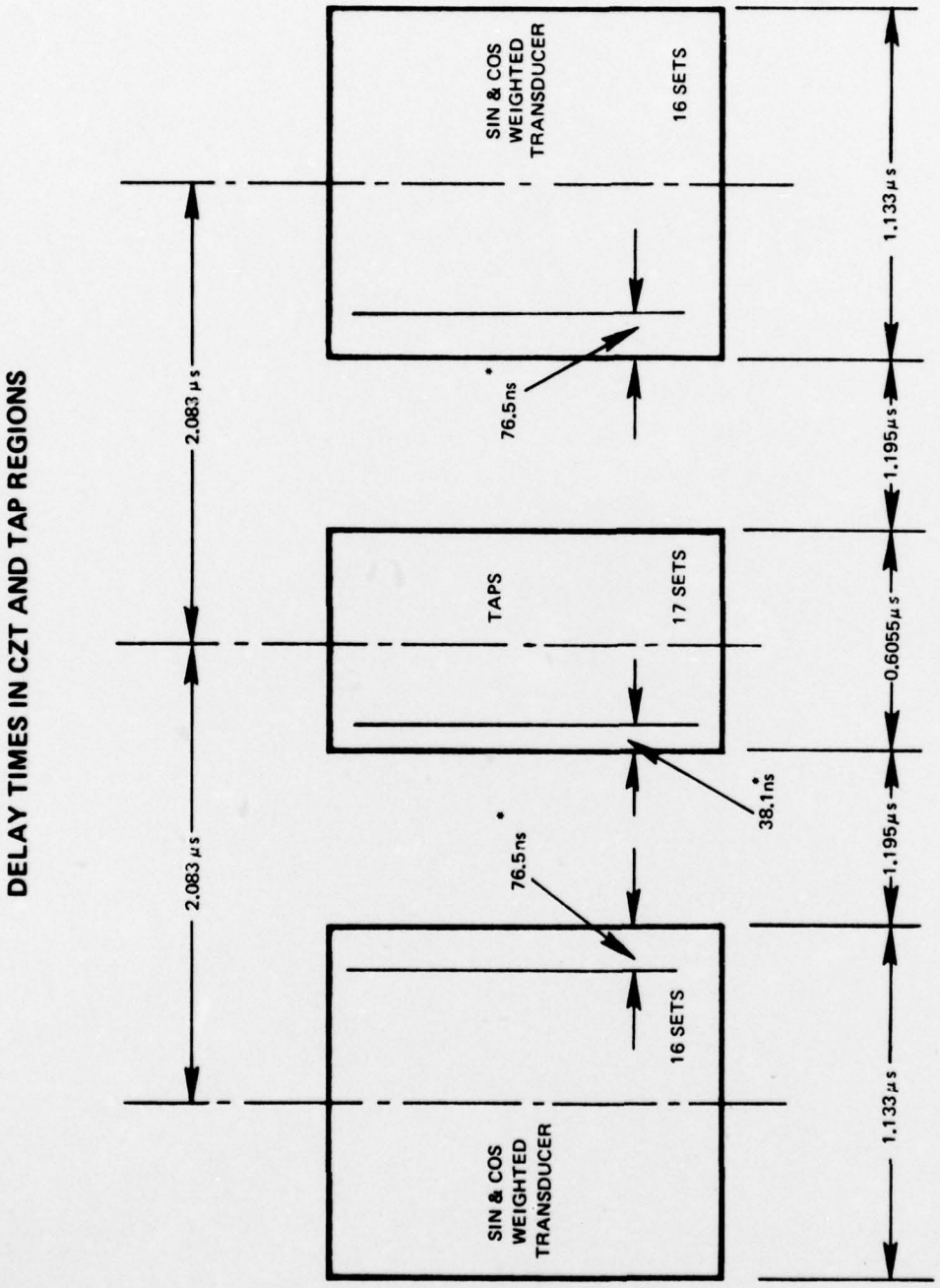

76-08-132-1

PHOTOGRAPHS OF THE SOS DIODE ARRAY

a) OVERALL VIEW

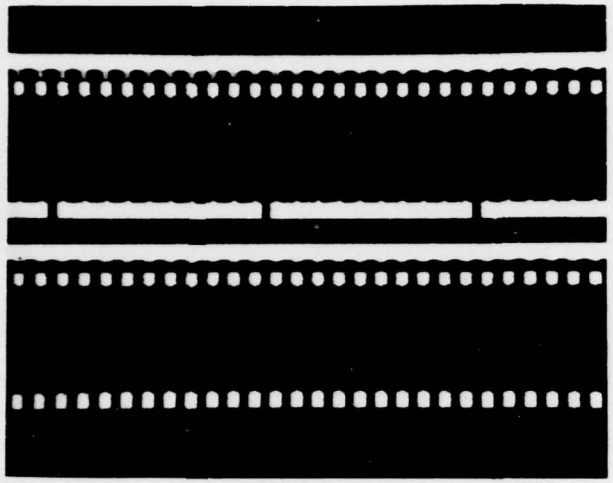

b) CLOSE-UP OF DIODES SPACED BY 0.005 IN.

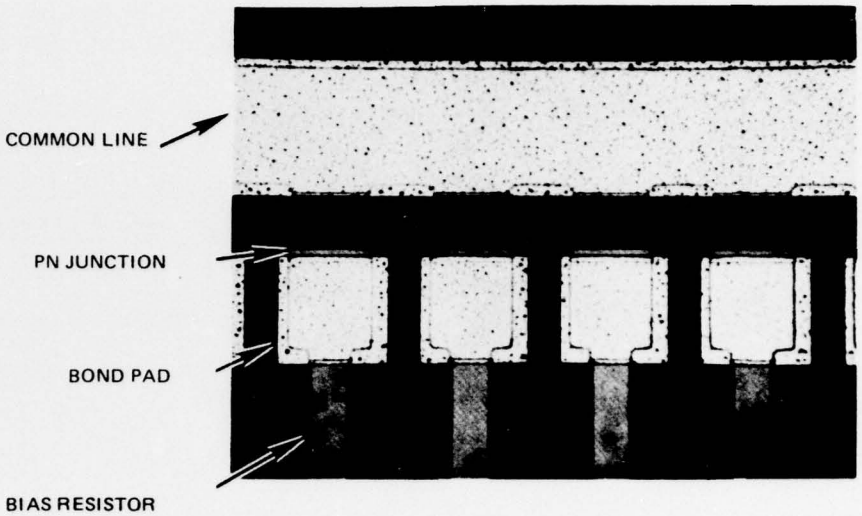

FIG. 4-5

FIG. 4–6

BLOCK DIAGRAM OF CHIRP SECTIONS USED WITH PULSE MODULATED RF SIGNALS

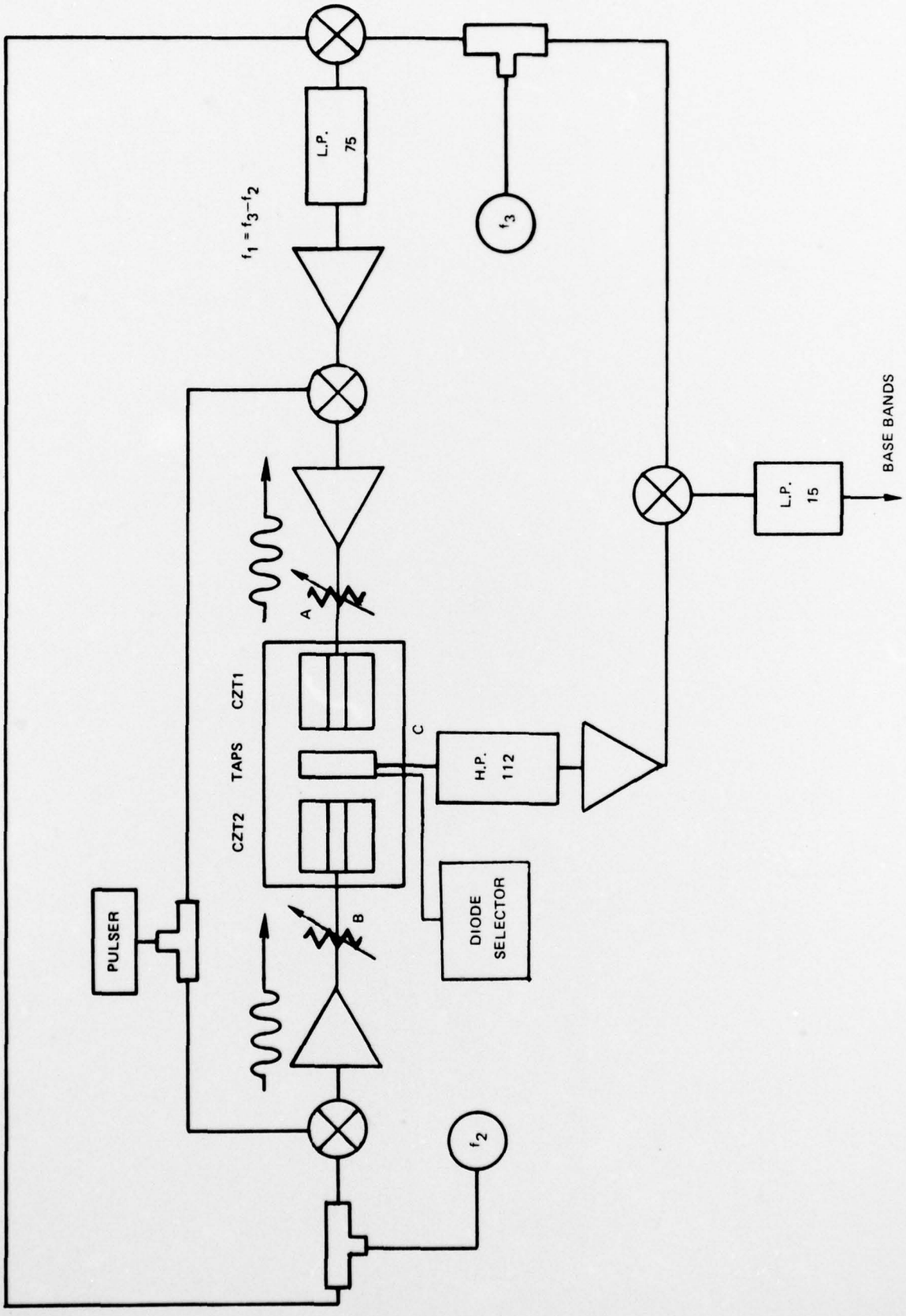

76–08–106–4

FIG. 4–7

SIGNALS FROM CZT TRANSDUCERS

f_1 = 61 MHz

f_2 = 86 MHz

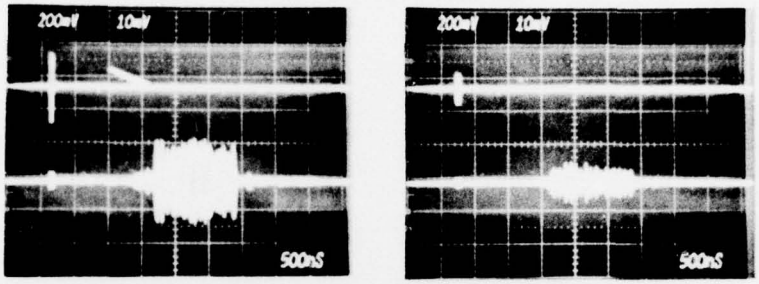

INPUT

CHIRP

CHIRP – SINGLE BURSTS

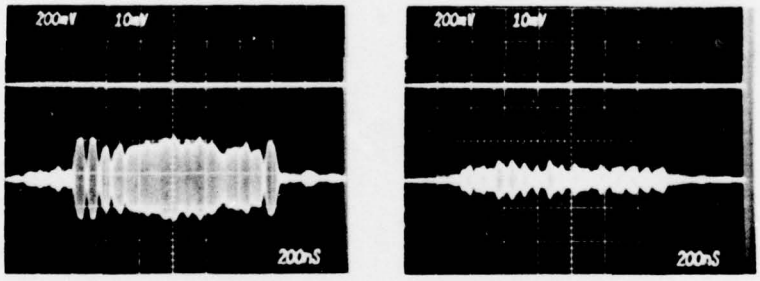

CHIRP – SINGLE BURSTS

(EXPANDED SCALE)

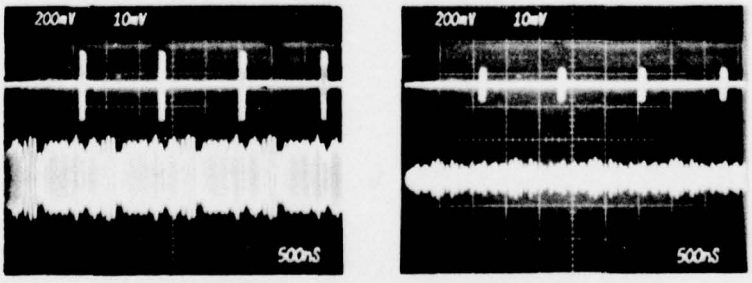

INPUT

CHIRP

CHIRP – CONTIGUOUS BURSTS

prf = 0.831 MHz

PULSE WIDTH = 90 ns

76–08–126–3

FIG. 4–8

CZT LINEAR OUTPUT SIGNALS AT VARIOUS TAPS WITH SINGLE PULSE INPUT AT BOTH f_1 AND f_2 TRANSDUCERS

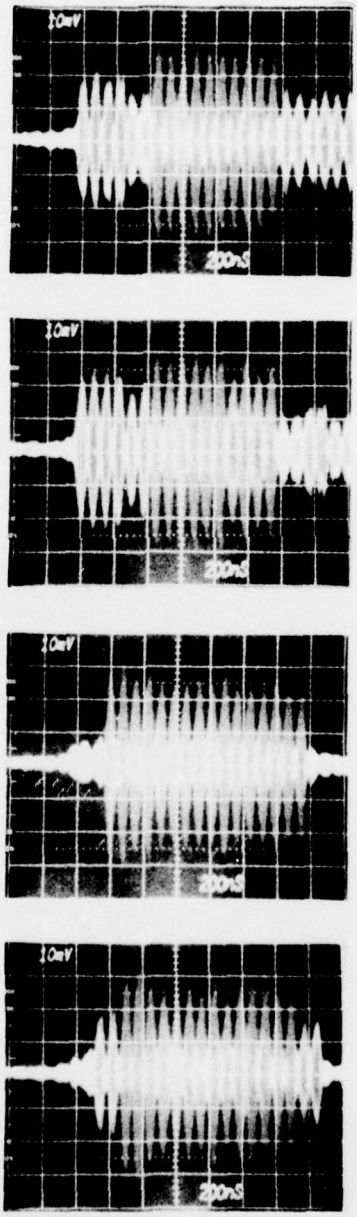

f_1 = 57MHz

f_2 = 85MHz

PULSED RF ~ 50ns

76–08–132–4

CZT LINEAR OUTPUT WITH ALL TAPS "ON" TO SHOW CORRELATION PEAKS

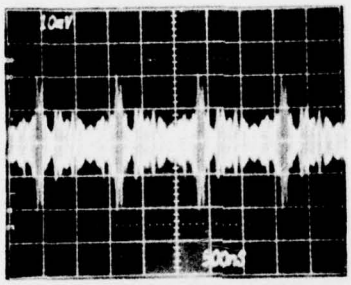

a) CORRELATION AT 57.18MHz

ALSO AT 59.63 MHz
58.81
57.98
57.18
56.36
55.58

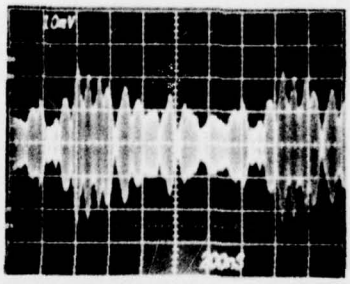

b) NON–CORRELATED AT 57.85 MHz

FIG. 4–10

BASE BAND SIGNALS USING PULSED RF SIGNALS TO DRIVE CZT'S (REF. TO TAP 9)

"0" BEAT AT TAP 9
f_3 = 146 MHz
f_2 = 85.5 MHz
f_1 = 60.5 MHz = $f_3 - f_2$

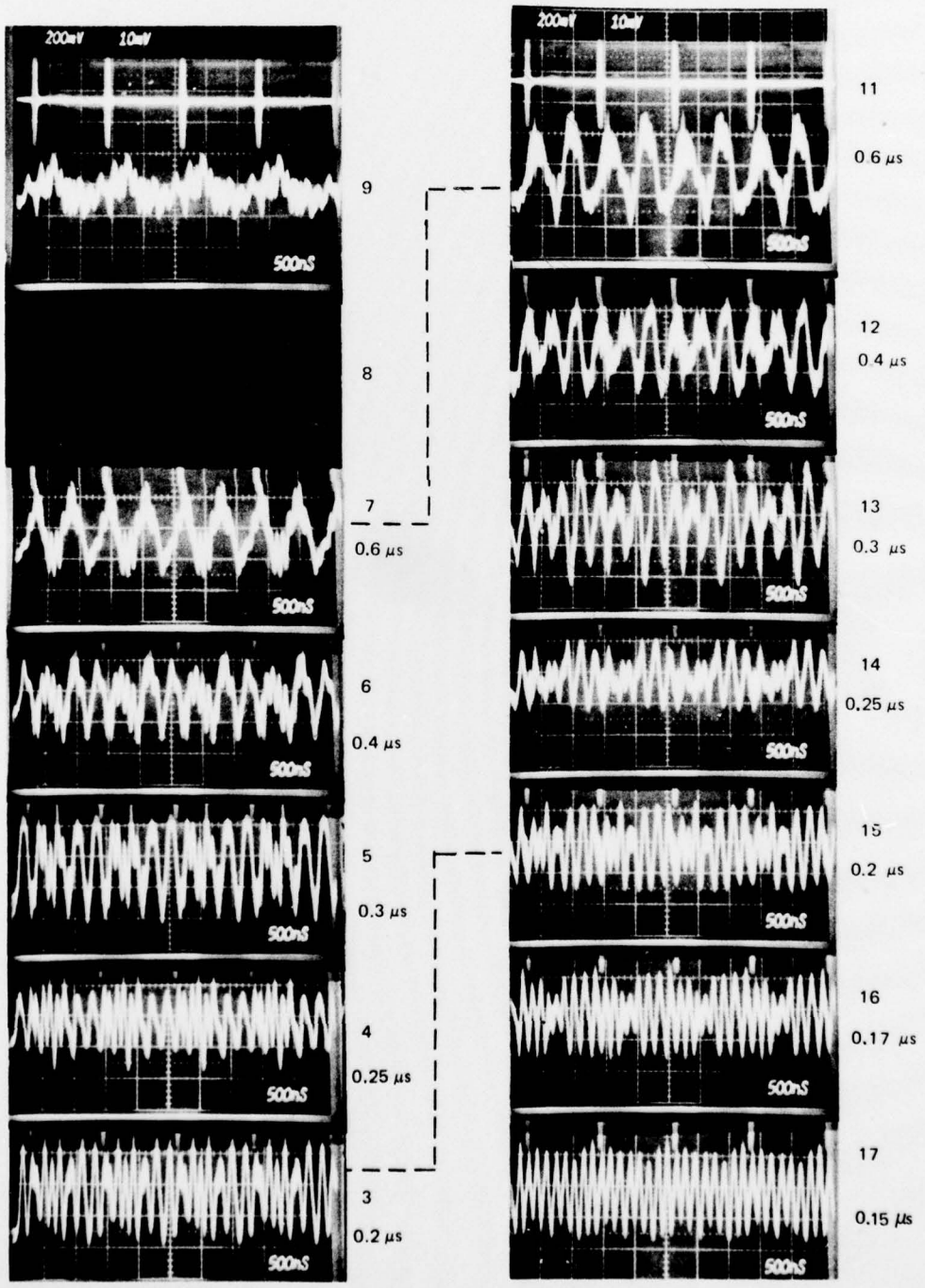

FIG. 4–11

BASE BAND SIGNALS USING PULSED RF SIGNALS TO DRIVE CZT'S (REF. TO TAP 17)

"0" BEAT AT TAP 17

f_3 = 1.39 MHz

f_2 = 85.5 MHz

f_1 = 53.5 MHz = $f_3 - f_2$

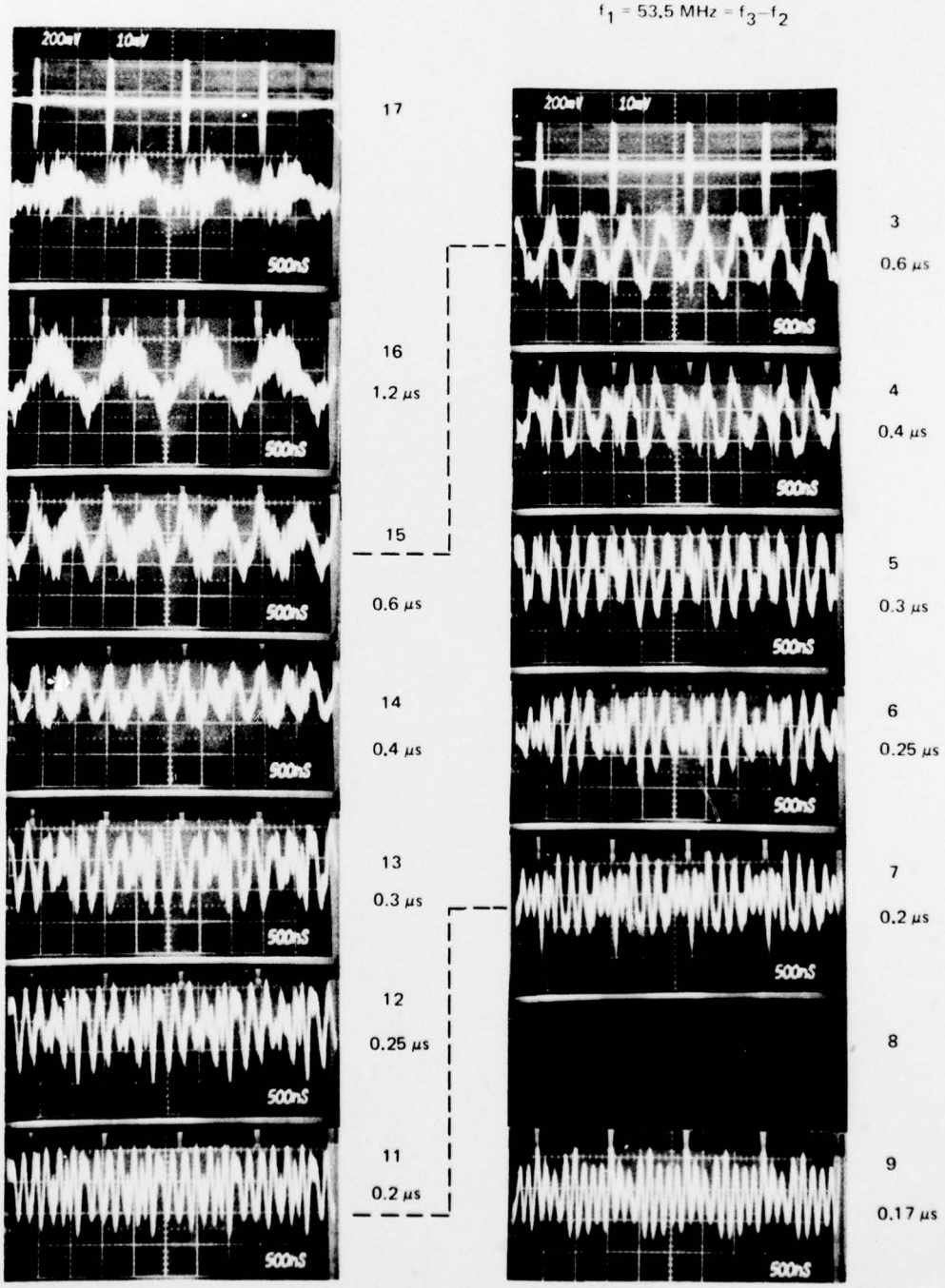

76–08–126–5

FIG. 4–12

BASE BAND SIGNALS USING MLSO'S TO DRIVE CZT'S

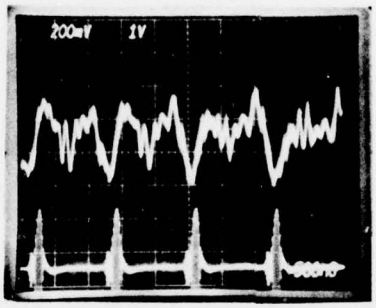

a) TAP 9

~ 1.7 MHz

PRF = 0.8378 MHz

PRF = 0.8378 MHz

L.O. FREQ = 144 MHz

f_1 ~ 62.5 MHz

f_2 ~ 85.4 MHz

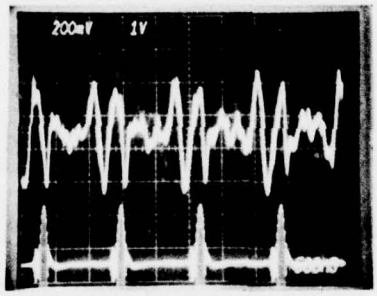

b) TAP 7

~ 3.3 MHz

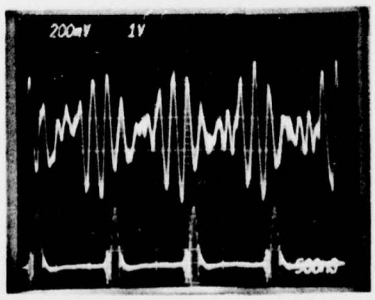

c) TAP 5

~ 5.0 MHz

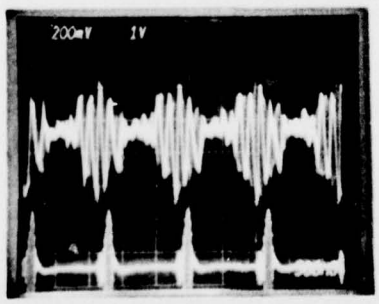

d) TAP 3

~ 6.7 MHz

FIG. 4-13

SAW CIRCUIT FOR FREQUENCY SYNTHESIS WITH CONTINUOUS CHIRPS

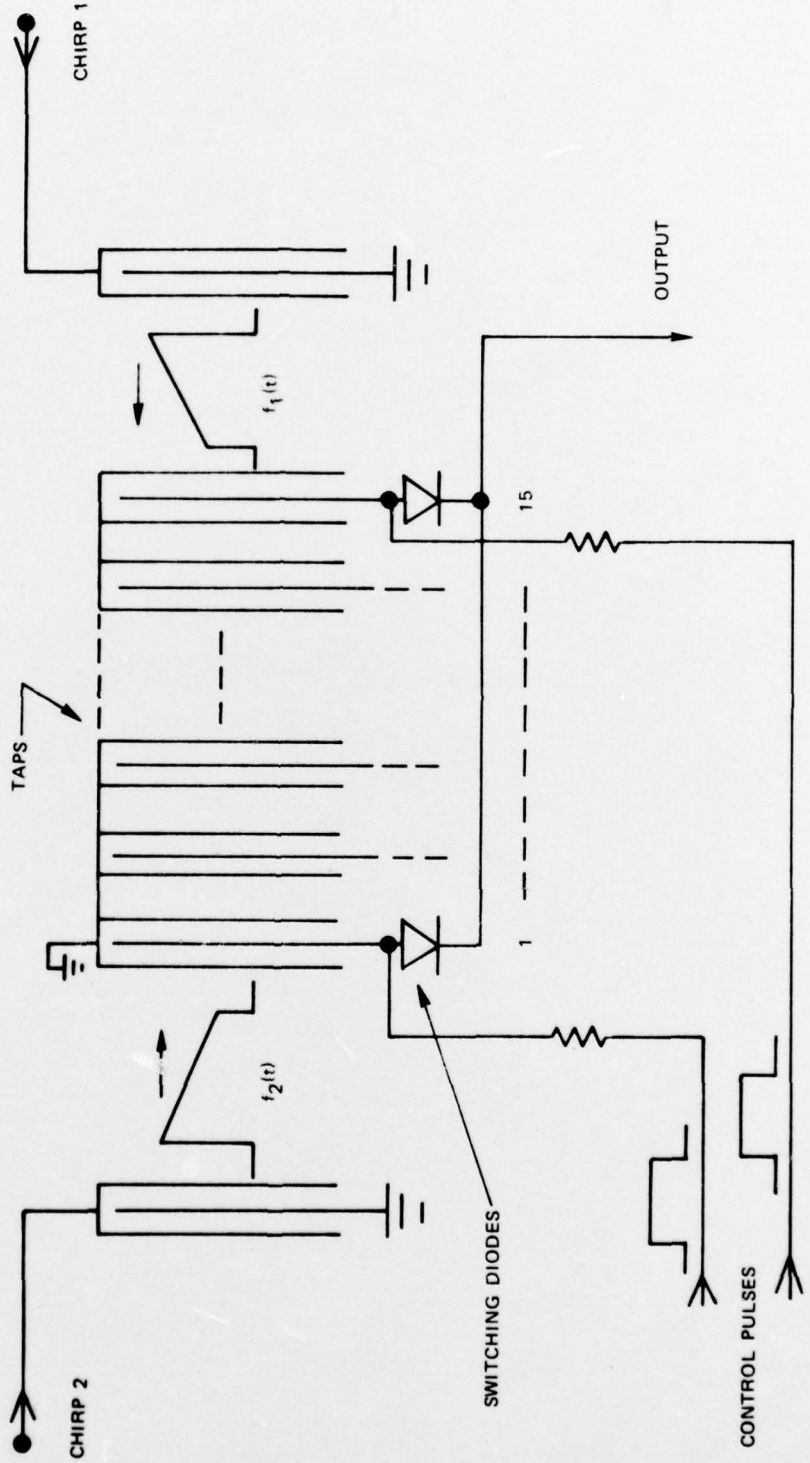

76-08-106-6

SYNTHESIZED SIGNALS FROM CONTINUOUS CHIRPS

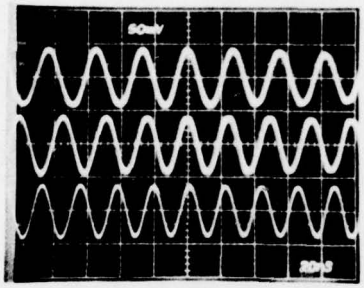

a) TYPICAL DIFFERENCE FREQUENCY SIGNALS I_b = 0.02 ma

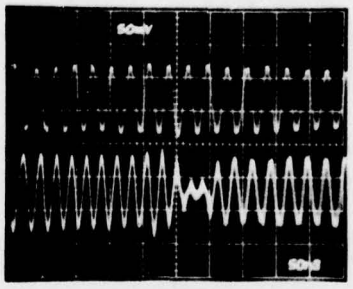

b) FREQUENCY SWITCHING

Distribution List

United Technologies Research Center Report No. R76-922155-3
Contract No. N66001-76-C-0011

Number Of Copies	
3	Receiving Officer (N66011)-76-C-0011 Naval Undersea Center South Rosecrans Street, Point Loma San Diego, California 92132 Code N66001
2	Mrs. Eleanor D. Solan Naval Undersea Center South Rosecrans Street, Point Loma San Diego, California 92132 Code 85221
2	Requesting Department Naval Undersea Center South Rosecrans Street, Point Loma San Diego, California 92132 Code 6000
2	Naval Undersea Center South Rosecrans Street, Point Loma San Diego, California 92132 Code 1112
5	Naval Plant Representative Office United Technologies Corporation Pratt & Whitney Aircraft Division East Hartford, Connecticut 06108
1	U.S. Navy Regional Finance Center 937 Harbor Drive San Diego, California 92132 Code 60957

Number Of Copies	
1	Dr. Robert W. Means Naval Undersea Center South Rosecrans Street, Point Loma San Diego, California 92132 Code 602
1	Mr. Ervin F. Johnston, Esq. Office of Patent Counsel Naval Undersea Center South Rosecrans Street, Point Loma San Diego, California 92132 Code 96